APOLIPOPROTEIN C-I AND APOLIPOPROTEIN E PRODUCTION DURING ADIPOCYTE DIFFERENTIATION

by

Aivi T. Nguyen

A thesis submitted to the Faculty of the University of Delaware in partial fulfillment of the requirements for the degree of Honors Bachelor of Science in Biological Sciences with Distinction.

Spring 2009

APOLIPOPROTEIN C-I AND APOLIPOPROTEIN E PRODUCTION

DURING ADIPOCYTE DIFFERENTIATION

by

Aivi T. Nguyen

Approved: _____

Dr. David Usher, PhD.
Professor in charge of thesis on behalf of the Advisory Committee

Approved: _____

Dr. William Cain, PhD.
Committee member from the Department of Biological Sciences

Approved: _____

Dr. Sharon Rozovsky, PhD.
Committee member from the Board of Senior Thesis Readers

Approved: _____

Alan Fox, Ph.D.
Director, University Honors Program

ACKNOWLEDGMENTS

As the adage goes, “It takes a whole village to raise a child.” I thank the following people for rearing, raising, and sometimes goading me into becoming who I am today:

- **Dr. David Usher**, for not only mentoring and guiding me but also molding my determination and attention to detail. I imagine my journey from when I first started sophomore year to now was much like watching a baby take its first steps—thank you for your limitless patience and support!
- **Dr. William Cain**, for showing me the in-and-outs of the lab and being a great mentor and friend. Also thank you for putting up with my endless “office pop-ins” for “one last question,” which was, of course, never the last question
- **Dr. Sharon Rozovsky**, for being possibly the most patient 3rd reader
- **Marysol Lavander**, for being a shoulder to lean on and lab mentor
- **Dr. Gary Laverty, Meg Meiman, Aravindan Rolands, Brian Danysh,** and **Lauren Isaacs**, for supplying the last leg of my project in both materials and moral support
- All my loved ones, **Chris Elder (Samwise), Richard Duong, Sharon Young,** and **Amber Majid**, for wanting to be my friend even after my curious disappearance senior year
- **My family**, for always loving and supporting me despite my HSPG-related tangents at every dinner
- **The Howard Hughes Medical Institute**, for scholarship support
- **The University of Delaware**, for providing just-the-right “milieu”

TABLE OF CONTENTS

LIST OF TABLES

LIST OF FIGURES

ABSTRACT

Cholesterol efflux, the process in which cells transport intracellular unesterified cholesterol to extracellular cholesterol acceptors, occurs late during adipocyte differentiation and involves secreted apolipoproteins which shuttle cholesterol to extracellular cholesterol acceptors. One apolipoprotein apoE produced by adipocytes, attaches to the cell surface through proteoglycan interactions, and plays an important role in cholesterol efflux to lipid poor HDLs. The Usher lab has discovered another apolipoprotein, apoC-I, which may also play a role in cholesterol efflux in adipocytes. The aim of this study is to (1) determine whether *Apoe* and *Apoc1* mRNA expression is dependent upon intracellular cholesterol levels; (2) detect secreted apoC-I from adipocytes; and (3) address whether apoC-I associates with heparan sulfate proteoglycans on the cell surface, like apoE. To measure *Apoe* and *Apoc1* mRNA expression Quantitative Real-Time PCR (QPCR) was used. Mouse 3T3-L1 fibroblasts were stimulated to differentiate and either not treated or treated with LXR agonist T0901317, β-cyclodextrin, serum-free media, or Intralipid. To access human APOC-I protein production, human adipocytes were grown on glass cover slips. The cover slips were either left untreated or treated with heparinase or heparinase and cell permeabilization. Cells were then visualized with rabbit anti-human APOC-I IgG and fluorescein isothiocyanate (FITC)-conjugated goat IgG. QPCR results demonstrated

that *Apoe* mRNA expression reaches a maximum during on Day 3 of differentiation, or intermediate-phase differentiation while maximum *Apoc1*mRNA expression occurs on Day 6 of late-phase differentiation.LXR agonist treatments increased expression of both *Apoe* and *Apoc1* mRNA, while cholesterol depletion with β-cyclodextrin and HDL decreased expression. Results indicated that *Apoc1* and *Apoe* mRNA expression is sensitive to cholesterol levels. Epifluorescence microscopy revealed that human APOC-I is produced during late-phase differentiation (Day 6) on the adipocyte surface in a distinct punctate pattern. Moreover, after heparinase treatments, little APOC-I was visualized, suggesting that APOC-I attaches to heparan sulfate proteoglycans on the cell surface. APOC-I production during adipocyte differentiation and subsequent binding to heparan sulfate proteoglycans on the adipocyte surface suggests that it may act as a cholesterol acceptor in potential lipid rafts, similar to apoE.

Chapter 1

INTRODUCTION

1.1 Obesity and Health Related Risks

Currently, obesity remains the number one leading preventable death in the developed world and afflicts 1.1 billion adults and 10% of children worldwide (Haslam & James, 2005). The condition is characterized by a body mass index of > 30 kg/m2 and is, moreover, the harbinger of numerous diseases: type II diabetes, coronary artery disease, osteoarthritis, and metabolic syndrome. Not only does obesity reduce life expectancy by 7 years by the age of 40, but research has demonstrated that it increases morbidity and mortality rates (Bays, 2009).

1.2 Obesity as a Function of Adipogenesis

Obesity is now recognized as an energy imbalance and remains a function of adipose tissue hypertrophy and hyperplasia, and ultimately, adipogenesis. When caloric intake, whether in the form of carbohydrates,fats, or protein, exceeds energy expenditure, excess energy is stored as fat in adipose tissue, specifically adipocytes. First, adipose tissue mass is dictated by adipogenesis, which is the proliferation and differentiation of preadipocytes to form more adipose tissue. Following differentiation,

adiposity then remains a function of adipocyte growth, or hypertrophy, and accrual of adipocyte number, or hyperplasia.

1.3 Regulation of Adipocyte Size

The formation of intracellular lipid droplets, a process known as lipogenesis, determines adipocyte size and indirectly hypertophy. Recently, lipid droplets have been recognized as a dynamic intracellular organelle, continuously re-modeling the lipid-filled interior and droplet surface proteins (Listenberger, Ostermeyer-Fay, Goldberg, Brown, & Brown, 2007). The lipid droplet core is predominantly comprised of triglycerides and esterified cholesterol (Ducharme & Bickel, 2008). The surface, however, is constructed of a phospholipid monolayer interspersed with unesterified, or free, cholesterol and a heterogeneously-spaced coat of the PAT family lipid droplet proteins: perilipin, adiophilin/adipocyte differentiation-related protein (ADRP), tail-interacting protein of 47 kilodaltons (TIP47), S3-12, and oxidative tissues-enriched PAT protein (OXPAT) (Brasaemle, 2007). Perilipin is the predominate protein surrounding the lipid droplet and, under basal conditions, acts as a barrier to cytosolic lipases which ultimately promotes triacylglycerol formation from free fatty acids and storage. However, under lipolytic stimuli, perilipin becomes phosphorylated by protein kinase A and grants adipose triglyceride lipase and hormone-sensitive lipases access to the lipid droplet interior. ADRP and TIP47, though less well-studied, have been shown to function similar to perilipin. Thus, studies on the PAT family lipid

droplet proteins have demonstrated the importance of fatty acid accumulation in dictating adipocyte size and adipose tissue mass.

In addition to the PAT family of lipid droplet proteins in regulating triglyceride accumulation into lipid droplets, intracellular cholesterol levels are also important in controling lipid droplet and ultimately adipocyte size. In adipocytes, cholesterol and triglyceride levels exhibit a proportional relationship—as triglyceride levels increase, both esterified and unesterified cholesterol levels also increase (Le Lay, Ferre', & Dugail, 2004). Studies have shown, when adipocytes are depleted of triglycerides, cholesterol content also decreases; as aforementioned, since cholesterol comprises the lipid droplet membrane, total adipocyte size also decreases as a consequence of diminished cholesterol levels. Subsequently, because triglycerides and esterified cholesterol comprise the lipid droplet interior while unesterified cholesterol constructs the droplet surface and adipocyte membrane, both are important factors in controlling the lipid droplet core lipid content and adipocyte size (Imamura, et al., 2002). Although both lipids influence one another and concomitantly dictate adipocyte size, cholesterol comprises the lipid droplet interior, lipid membrane, and cell plasma membrane, which demonstrates that it may ultimately play a larger role in dictating adipocyte size. Thus, cholesterol homeostasis—the dynamic process involving cholesterol synthesis, influx, and efflux—within the adipocyte proves important.

1.4 Cholesterol Homeostasis in Adipocytes

1.4.1 Cholesterol Synthesis and Influx

Cholesterol synthesis is one way in which adipocytes increase intracellular cholesterol levels during periods of cholesterol depletion. During periods of sterol abundance the sterol-responsive element-binding protein 2 (SREBP-2), a transmembrane protein located on the endoplasmic reticulum (ER) membrane, avidly binds to SREBP cleavage activating protein (SCAP) and Insig-1 which act as both a sterol sensor and anchor to the ER. However, once cholesterol levels drop beneath 5% of its basal production, Insig-1 dissociates from the protein complex, allowing the resulting SCAP-SREBP-2 proteins to bud off to the Golgi for further processing. At the Golgi, SREBP-2 undergoes a sequential two-step cleavage by the S1P and S2P proteases, which liberate the NH-2 terminal domain. Upon release, SREBP-2 then translocates to the nucleus and ultimately acts as a transcription factor by binding to the sterol-responsive elements (SREs) associated with a myriad of gene promoters involved in cholesterogenesis, the most pertinent being 3-hydroxy-3-methylglutaryl-coenzyme A reductase (HMG CoA reductase). Since HMG CoA reductase is the rate-limiting enzyme in the cholesterol synthetic pathway, up-regulation of transcribed HMG CoA reductase increases cholesterol synthesis (Radhakrishnan, Goldstein, McDonald, & Brown, 2008; Inoue, Kumagai, Terada, Maeda, Shimizu, & Sato, 2001)

Another gene which SREBP-2 acts as a transcription factor for is the low-density lipoprotein receptor (LDLR). Following transcription and translation, LDLR is

expressed on the cell surface and sequesters exogenous cholesterol through binding the cholesterol-rich plasma lipoprotein, LDL, and triglyceride rich lipoproteins, IDL, VLDL and chylomicrons. LDLRs bind lipoproteins through recognition of apolipoprotein B100 (apoB) on low density lipoproteins (LDLs), or apolipoprotein E (apoE) found on chylomicron remnants, very-low density lipoproteins (VLDLs). Once bound, the lipoproteins undergo receptor-mediated endocytosis wherein cholesterol is utilized for the cell. LDLR expression is controlled in part through the sterol-sensitive expression of PCSK9 gene, which transcribes specific proteinases that lead to the degradation of LDLR (Attie & Seidah, 2005). This shows that both cholesterol synthesis and enhanced uptake contribute to increasing intracellular cholesterol levels within adipocytes.

1.4.2 Cholesterol Efflux

Another important aspect of adipocyte cholesterol homeostasis is the exodus of excess intracellular cholesterol from the cell, termed cholesterol efflux. Cholesterol efflux encompasses the transfer of intracellular unesterified cholesterol from the cell plasma membrane to an extracellular lipid acceptor. It involves a number of proteins including the transmembrane ATP-binding cassette transporters A1 and G1 (ABCA1 and ABCG1, respectively), scavenger receptor BI (SR-BI), and high density lipoproteins (HDLs) which are the extracellular cholesterol acceptors (de la Llera-Moya, et al., 2001).

ABCA1 and ABCG1 belong to a family of transmembrane proteins which transfer various molecules across the cell membrane by hydrolyzing ATP for energy. Specifically, ABCA1, a full transporter containing two transmembrane domains (TMs) and two nucleotide-binding folds (NBFs), promotes the unidirectional flux of free cholesterol to lipid-free or lipid-poor HDLs. Meanwhile, ABCG1, a half-transporter with one TM and NBF, works in tandem with ABCA1 but has been shown to efflux cholesterol to lipid-rich acceptors particles (Adorni, et al., 2007).

Lastly, SR-BI also facilitates cholesterol efflux to extracellular acceptors. Unlike ABCA1 and ABCG1, SR-BI mediates a bi-directional flux of cholesterol; however, like ABCG1, SR-BI associates with mature, lipid-laden HDLs (Gelissen, et al., 2006).

1.4.3 Reverse Cholesterol Transport

Coupled with cholesterol influx, synthesis, and efflux, reverse cholesterol transport (RCT) proves essential in maintaining dynamic cholesterol homeostasis in the cell and in the body. As aforementioned, adipocytes efflux free cholesterol onto extracellular cholesterol-acceptors like HDLs using transmembrane protein mediators such as ABCA1, ABCG1, or SR-BI. In RCT, HDLs ultimately transport the effluxed cholesterol from peripheral cells to the liver for catabolism, since non-hepatic cells are unable to catabolize cholesterol themselves (Yancey, Bortnick, Kellner-Weibel, de la Llera-Moya, Phillips, & Rothblat, 2003). Like most peripheral cells, adipocytes produce and secrete specific apolipoproteins which are the purported mediators of cholesterol transport between the cell and HDL particles. Moreover, current research

has demonstrated that apolipoproteins also aid in lipoprotein biogenesis or modulate particle size. Particularly, apolipoproteins E (apoE) has been identified as important in cholesterol efflux (Mahley, Huang, & Weisgraber, 2006), and both apoE and C-I (apoC-I) play an active role in RCT, and lipoprotein metabolism (Adorni, et al., 2007; Westerterp, et al., 2007).

1.5 Apolipoproteins E and C-I in Adipocytes

1.5.1 Function and Regulation of Apolipoprotein E

An apolipoprotein that plays a significant role in cholesterol efflux is apolipoprotein E (apoE). Unlike most apolipoproteins, apoE, a 33-37 kDa glycoprotein, has been shown to be secreted by cells outside the enterohepatic axis, the intestinal- and liver-associated lipoprotein path to clearance, particularly by macrophages and adipocytes (Laffitte, et al., 2001).

In adipose tissue, apoE functions primarily as a lipid modulator in adipocytes. Specifically, apoE has been shown to be involved in cholesterol efflux to lipid-poor HDL_3, or lipid-free apolipoproteins apoA-I by interacting with ABCA1 (Gelissen, et al., 2006).Other research, however, has also shown that apoE can participate in cholesterol efflux in macrophages independent of ABCA1, suggesting alternate cholesterol efflux mechanism (Huang, Lin, Oram, & Mazzone, 2001). Regardless, it is unknown whether endogenously produced or exogeneous, HDL-associated apoE facilitates in cholesterol efflux (Dove, Linton, & Fazio, 2004).Ultimately, apoE

expression is observed during late adipocyte differentiation, indicating its role in adipocyte lipid accumulation and homeostasis (Carmel, Tarnus, Cohn, Bourdon, Davignon, & Bernier, 2009).

In adipocytes, apoE production is tightly controlled by cellular cholesterol content, particularly free cholesterol. Previous research has established the cholesterol-dependent expression of *Apoe* mRNA during adipocyte differentiation. In a studied conducted by Zechner et al. (1990), *Apoe* mRNA levels mirrored free cholesterol levels: *Apoe* mRNA decreased during cholesterol depletion and biotin depravation and increased during cellular loading of exogenous free cholesterol. Additional studies have verified the sterol-dependent gene transcription and have also elucidated the molecular control mechanisms. Upon lipid accumulation or increased intracellular sterol levels, nuclear receptor liver X receptor A (LXRα), a ligand-activated nuclear transcription factor, dimerizes with retinoic X receptor (RXR). Upon dimerization, LXR/RXR interacts with the LXR responsive element (LXRE) located on two enhancers multienhancer 1 (ME.1) and multienhancer 2 (ME.2) which flank the *Apoe* gene. Once the LXREs on ME.1 and ME.2 are activated, transcription of the *Apoe* gene occurs. Thus, through the sterol-sensing control of LXR, *Apoe* expression occurs late in adipocyte differentiation and further limits the extent of lipid accumulation through cholesterol efflux (Laffitte, et al., 2001).

In addition to mediating cholesterol efflux, apoE is also heavily involved in RCT and lipoprotein metabolism. ApoE has been shown to associate with chylomicron remnants, VLDL, and certain subclasses of HDLs and acts primarily as a ligand for

LDLRs located on the liver (Figure 1.1). When associated with the LDLR, apoE promotes the hepatic clearance of the plasma lipoprotein particle, which ultimately reduces plasma cholesterol levels, through receptor-mediated endocytosis. Specifically, apoE has been shown to associate with heparin and heparan sulfate proteoglycans (HSPG) on hepatocyte surfaces in the spaces of Disse. In particular, the 22-kDa NH2-terminal domain (residues 1-191) contains the necessary lysine and arginine residues (spanning 140-150) which hydrogen bond with N-, 2-O-, and 6-O-sulfo groups on heavily sulfated heparin glucosamine chains (Figure 1.2).

More importantly, this apoE-HSPG interaction facilitates apoE binding to LDLRs or LDLR-related proteins (LDLR), thereby aiding hepatic uptake of various apoE-expressing lipoproteins. Though apoE is mostly produced in the liver, specifically at the spaces of Disse, abundant apoE-HSPG interactions have also been shown in macrophages and astrocytes (Lucas & Mazzone, 1996). Lucas and Mazzone (1996) demonstrated that macrophage-secreted apoE associates with HSPG and, furthermore, modulates net cell apoE production. Additionally, aside from abundant expression in macrophages and hepatocytes, apoE-HSPG interactions have just recently been shown in astrocytes as well and are implicatd in the development of Alzhiemer's plaque in the brain (Libeu, et al., 2001).

In addition to interacting with the cell surface, research has shown that apoE is secreted as a water-soluble protein capable of binding a variety of lipoproteins. ApoE exhibits the ability to bind VLDL and HDL_3, a subclass of HDLs, transfer between the two lipoproteins, depending on its binding affinity, thereby affecting hepatic uptake

and altering specific peripheral cell and lipoprotein interactions. Ultimately, whether secreted or bound, apoE functions as an important protein involved in lipoprotein biogenesis and plasma clearance of various lipoprotein particles (Nguyen, Dhanasekaran, Phillips, & Lund-Katz, 2009).

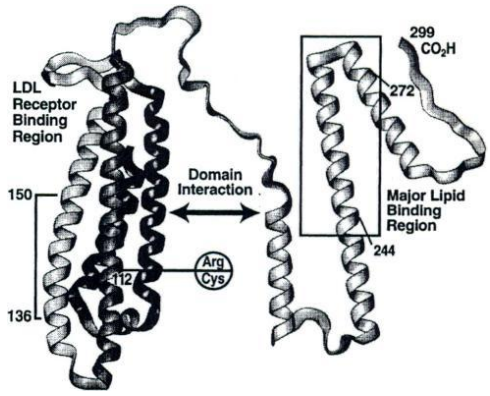

Figure 1.1. Binding Domains in APOE. (Image source http://www.fasebj.org/cgi/reprint/10/13/1485)

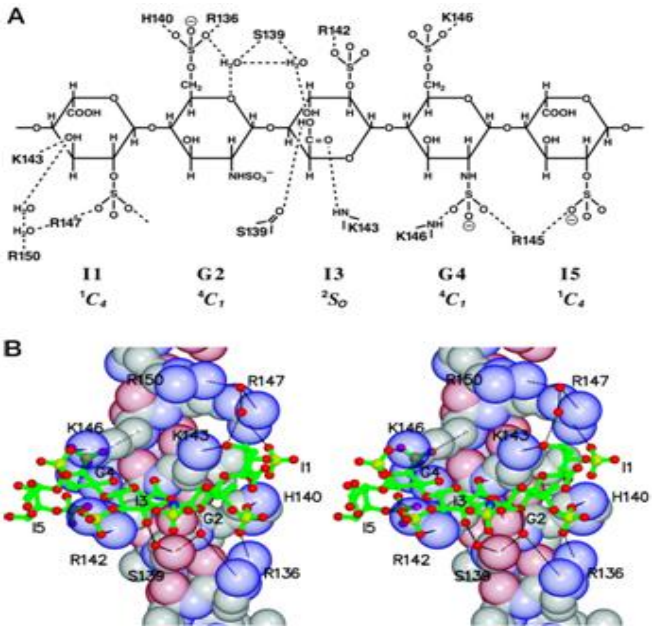

Figure 1.2. APOE and Heparan Sulfate Proteoglycan Interactions. (A) Heparan sulfate interactions with APOE lysine and arginine residues (B) Ball-and-stick model of heparan sulfate interaction with APOE. (Image source: http://www.jbc.org/cgi/content/full/276/42/39138)

1.5.2 Function and Regulation of Apolipoprotein C-I

Another less-studied apolipoprotein that may be involved in cholesterol efflux and RCT is apoC-I. ApoC-I is a 57-amino acid protein (6.6 kDa) expressed by hepatocytes, glial cells, astrocytes, endothelial cells, and just recently, adipocytes.Similar to apoE, apoC-I typically associates with chylomicron remnants, VLDL, and HDLs. Although little is known in terms of apoC-I function in cholesterol efflux, it is speculated that apoC-I interacts with ABCG1 to efflux cholesterol to HDL particles (unpublished, David, 2006; unpublished, Sterling, 2007). Since triglyceride-rich HDL_2 particles engorged with esterified cholesterol is hypothesized to interact with ABCG1, it is possible that apoC-I also interacts with HDL_2 particles as well.

Research has established apoC-I's importance in RCT and lipoprotein metabolism. First, apoC-I interferes with apoE-dependent hepatic uptake of VLDL and HDL, ultimately leading to increased plasma lipid levels (Kowal, Herz, Weisgraber, Mahley, Brown, & Goldstein, 1990). In one study, overexpression of apoC-I in LDLR-knockout mice led to increased plasma cholesterol and trigylcerides when compared to control LDLR-knockout mice (Jong, Hofker, & Havekes, 1999). Moreover, inhibited LDLR-lipoprotein binding was attributed to apoC-I interfering with apoE-mediated binding of lipoproteins to LDLRs or LDLR-related protein (LRP) (Kowal, Herz, Weisgraber, Mahley, Brown, & Goldstein, 1990). Whether apoC-I inhibits apoE binding by masking the apoE receptor domain or displacing apoE from the lipoprotein particles remains uncertain. Ultimately, apoC-I expression interferes with apoE-mediated binding of VLDLs and HDLs to hepatic receptors, thus leading to impaired hepatic plasma lipoprotein clearance and possibly hyperlipidemia.

In addition to modulating plasma lipoprotein uptake, apoC-I regulates important enzymes involved in lipoprotein metabolism, specifically HDL anabolism, such as lecithin-cholesterol acyl transferase (LCAT) and cholesterol acyl transferase protein (CETP). ApoC-I activates LCAT, a major enzyme which esterifies free cholesterol present on circulating HDL. Moreover, LCAT is responsible for transforming the subclass of small, dense HDLs (HDL_3) into the larger HDL_2 particle. Thus, apoC-I activation of LCAT promotes HDL biogenesis and re-modeling through cholesterol esterification, which allows cholesteryl esters to accumulate in the HDL core (Hoeg, et al., 1996). While apoC-I activates LCAT, it has also been shown to be a potent,

highly selective inhibitor of CETP (Gautier, et al., 2000). CETP facilitates the equimolar exchange of neutral lipids, like cholesteryl esters and triglycerides, between various plasma lipoproteins. For instance, CETP mediates a bi-directional lipid flux between HDLs and triglyceride-rich particles or apoB-containing lipoprotiens like VLDLs and LDLs or between two separate HDL subclasses, ultimately altering HDL lipid content. Because CETP exchanges cholesteryl esters from HDL for triglycerides on VLDLs and LDLs, HDLs become triglyceride-rich and cholesterol-poor. Moreover, CETP arbitrates triglyceride transfer between large, lipid-rich HDL_2 particles to small, dense HDL_3 particles destined for catabolism in the liver. ApoC-I inhibition of CETP, then, significantly attenuates lipid transfer between lipoproteins and ultimately increases triglyceride content on HDLs. Thus, through LCAT activation or CETP inhibition, apoC-I partly transforms HDL lipid profiles and may partake in dynamic HDL remodeling (Gautier, et al., 2002). Interestingly CETP is not expressed in rodents (Ha & Barter, 1985).

Although little is known about apoC-I regulation, the close proximity of *Apoe* and *Apoc1* on the same gene cluster on mouse chromosome 7 and human chromosome 19 suggest coordinate regulation. Similar to *Apoe* mRNA expression, previous research has shown that *Apoc1* mRNA levels are highly upregulated during late phase human and mouse adipocyte differentiation; moreover, LXR agonists, the cholesterol-dependent nuclear transcription factor controlling the *Apoe* gene, upregulated *Apoc1* mRNA expression also mirrored in *Apoe* mRNA levels. Thus, like *Apoe*, *Apoc1* may

be sensitive to intracellular sterol levels, especially in adipocytes (unpublished, David, 2006; unpublished, Sterling, 2007).

1.6 Hypothesis and Experimental Approach

The purpose of this study is to verify previous data from the Usher lab regarding *Apoe* and *Apoc1* mRNA expression and also to determine *Apoc1* protein production in human adipocytes during differentiation. Specifically:

- Is *Apoc1* mRNA expression regulated by the cell's cholesterol content
- Are APOC-I and APOE produced and secreted by human adipocytes during late-phase adipocyte differentiation
- Is APOC-I associated with the adipocyte surface by binding heparan sulfate proteoglycans

It is first hypothesized that *Apoc1* mRNA levels are sensitive to intracellular cholesterol levels, like *Apoe* mRNA expression, and thus will be sensitive to LXR agonist T0901317 treatments in differentiated adipocytes. Concordantly, cholesterol depletion using β-cylcodextrin and HDL should show the opposite effect and decrease *Apoc1* mRNA levels. Second, since previous research by the Usher Lab has shown that *Apoe* and *Apoc1* mRNA levels are highly upregulated during late-phase differentiation, *Apoe* and *Apoc1* protein production will mirror the mRNA increase in a time-dependent manner. Lastly, since APOE has been shown to be secreted by adipocytes and also associate with cell-surface proteoglycans through lysine and

arginine interactions, secreted APOC-I should interact specifically with cell surface heparan sulfate proteoglycans.

To test the hypothesis both 3T3-L1 mouse and human adipocytes will be grown to confluency and induced to differentiation into adipocytes. Upon differentiation, cells will either be maintained with stimulated media, albeit in a quiescent state, or challenged with various treatments.

1.7 3T3-L1 Adipocyte and Human Subcutaneous Adipocyte Differentiation

The 3T3-L1 cell line, a pluripotent stem cell line isolated from Swiss mouse embryos, is a regularly used model for adipocyte differentiation. 3T3 cells originate from the embryonic mesoderm and are able to commit as either preadipocyte, cartilage, bone, or smooth muscle cells (Taylor & Jones, 1979; Ailhuad, et al., 1992). The 3T3-L1 cell line had been selected to specifically differentiate into adipocytes upon induction differentiation.

Cells are grown to confluency, which triggers the expression of a number of genes associated with growth arrest. Other expressed genes commit the cells to become preadipocytes. Differentiation is induced by the addition of a cocktail containing insulin, dexamethasone, and 3-isobutyl-1-methylxanthine.Adipocyte differentiation is demarcated by the appearance of lipid droplets, which stores fatty acids as triglycerides, and cell hypertrophy. The time course of adipocyte differentiation first entails cell division and DNA replication, which includes early and intermediate gene activation. Afterwards, transcription factors produced by intermediate genes stimulate

expression of late genes involved with growth arrest and lipid droplet formation beginning sometime between Day 3 to Day 7. 3T3-L1 preadipocytes are not fully mature until Day 9 following stimulation (Figure 1.3).

Human preadipocyte differentiation is induced 48 hours post-confluency and follows a differentiation pattern similar to mouse 3T3-L1 preadipocytes (Figure 1.3). Between 3 and 7 days post-differentiation lipid droplets form, indicating adipocyte maturation. By 14 days following differentiation, cells are fully mature with plentiful lipid droplets (Figure 1.4)

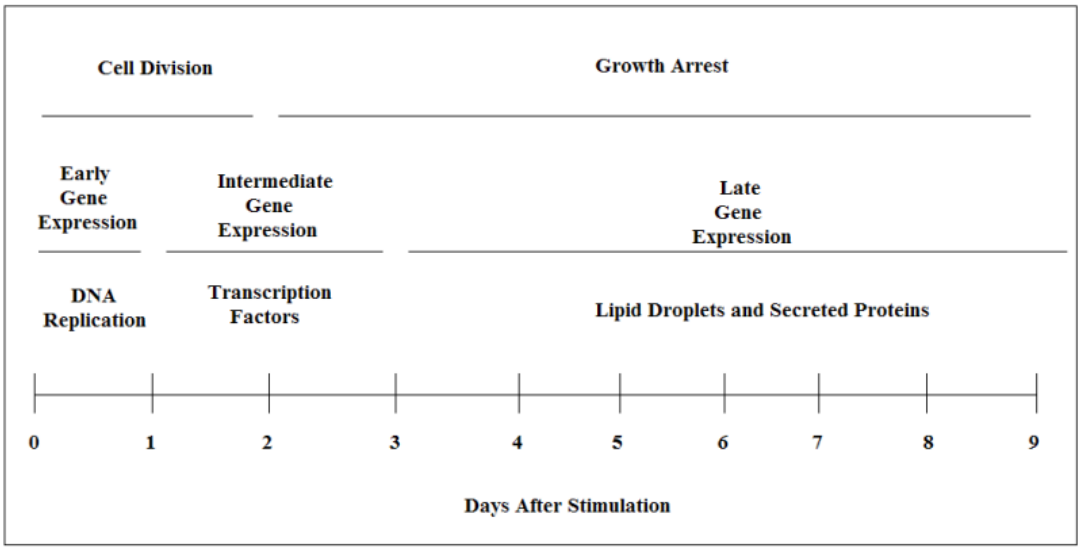

Figure 1.3. Adipocyte Differentiation and Expression of Genes Time-Course. Chart courtesy of John David, 2006.

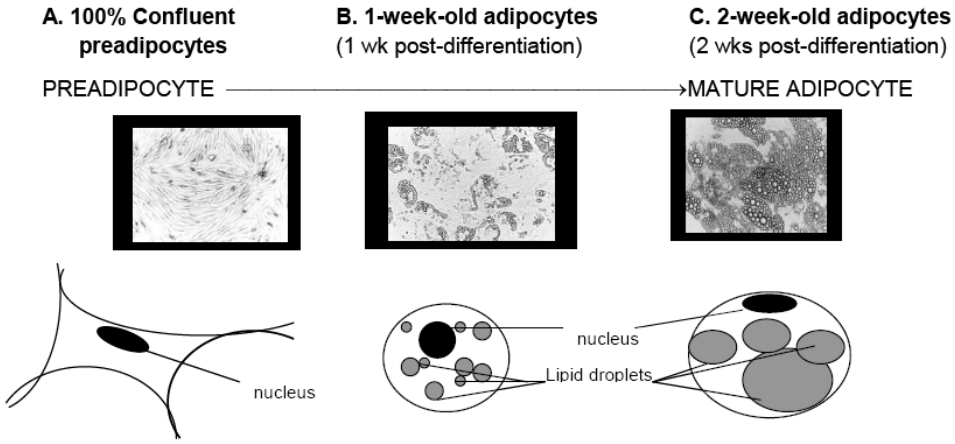

Figure 1.4. Human Subcutaneous Adipocyte Differentiation Cell Morphology and Time-Course. Image taken from ZenBio Adipcoyte Maintenance Manual.

Chapter 2

MATERIALS AND METHODS

2.1 HDL Preparation

HDL was obtained by ultracentrifugation of human plasma. Plasma sample densities were first adjusted to 1.21 g/mL using NaBr (Fisher Scientific, Fairlawn, New Jersey) and subsequently ultracentrifuged using a Ti60 Beckman rotor at 50,000 RPM for 43 hours at 15C. Afterwards, the lipoprotein fraction was collected and dialyzed twice against 1X PBS at 4C overnight. HDL concentrations were determined using absorbance at 280 nm and a BSA (Pierce Chemicals, Rockford, Illinois) standard at 2 mg/mL.

2.2 3T3-L1 Cell Culture

2.2.1 3T3-L1 Culture Conditions

3T3-L1 fibroblasts were purchased from ATCC (Manassas, Virginia) and thawed in a 37C water bath for 2 min. Afterwards, the vial was removed from the water bath and 1.5 mL of the contents were transferred to a 15 mL sterile conical tube with 9 mL of Growth Medium 1 (GM-1), containing DMEM with 10% calf serum (Invitrogen, Carlsbad, California), 1% L-glutamine (Mediatech Cellgro, Manassas, Virginia), and

1% penicillin/streptomycin (Mediatech Cellgro). Cells were spun at 125 x g for 5.5 min, and once the supernatant was discarded, the cell pellet was resuspended with 5 mL of GM-1 and seeded directly onto a T-25 flask. Cells were maintained in 5 mL of GM-1 at 37C and 5% CO2, with a media change every 48 hours. Upon reaching 60% confluency, the cells were treated with 0.75 mL of trypsin (Mediatech Cellgro, Manassas, Virginia) for 6 min. Afterwards, the total flask volume was brought to 15 mL with GM-1, and three T-75 flasks were seeded with 5 mL of the cell-media mixture. Once cells reached 70% confluency in T-75 flasks, cells were treated with 1.5 mL of trypsin. Afterwards, GM-1 was added to the flask, and 2 mL of the cell mixture was added to individual wells of nine 6-well plates. Cells were maintained in 2 mL of GM-1 at the standard culture conditions and observations as well as media changes were made every 48-72 hours until confluency was reached.

To differentiate the 3T3-L1 cell line, a standard 3T3-L1 differentiation protocol previously established by Yue et al (2004) was used, with minor modifications. Contact inhibition and conversion of adipoblasts to preadipocytes was insured by inducing 3T3-L1 differentiation 72 hours post-confluency (Day 0). Cells were washed 3 times with 1 mL of PBS per well of each 6-well plate, and 2 mL of inducing medium was added to each well. Inducing medium included 0.5mM 3-isobutyl-1-methylxanthine, 1 uM dexamethasone, and 10mg/mL insulin in Growth Medium 2 (GM2), which was comprised of DMEM, 10% fetal bovine serum, 1% L-glutamine, and 1% penicillin/streptomycin (Invitrogen). After 48 hours from inducing

differentiation, inducing medium was removed by washing cells twice with 1 mL of 1X PBS, and fresh GM2 was added to each well every 48 hours.

2.2.3 Serum-Free Media Treatment

Serum Free Media (Invitrogen) was added directly to 3T3-L1 cells on Day 5 of differentiation in lieu of GM-2 and changed daily, with 2mL of serum free media in each well. Treated 3T3-L1 cells were also monitored for lipid accumulation and viability.

2.2.4 Serum-Free Media and Intralipid Treatment

Intralipid treatments were prepared at 100 ug/mL in serum free media and 2 mL of the treatment media was added directly to 3T3-L1 cells on Day 5 of differentiation (Hadri, et al., 2004). Treatments were made fresh and changed daily, with 2 mL of treatment solution per well. Treated 3T3-L1 cells were also monitored for lipid accumulation and viability.

2.2.5 β-cylcodextrin/HDL Treatment

β-cylcodextrin (Sigma-Aldrich, St. Louis, Missouri) stock solutions were first made in distilled, de-ionized water (7.5 mM,425 mg of β-cylcodextrin in 50 mL of ddH20), and added to the cell culture media for a final concentration of 0.75 mM. HDL was added to the same medium at a final concentration of 1 mg/mL. The β-cylcodextrin/HDL treated media was added to 3T3-L1 cells on Day 5 of

differentiation, made fresh, and changed daily, with 2mL of treatment solution per well. Treated 3T3-L1 cells were also monitored for lipid accumulation and viability.

2.2.6 Stimulation of LXR Activity with T0901317

T0901317 (Cayman Chemicals, Ann Arbor, Michigan) stock solutions were first made in DMSO (3 mM, 10 mg T0901317 in 6.94 mL of DMSO), and added to the cell culture media for a final concentration of 3 uM. The T0901317 treated media was added to 3T3-L1 cells on Day 5 of differentiation, made fresh, and changed daily, with 2mL of treatment solution per well. Treated 3T3-L1 cells were also monitored for lipid accumulation and viability.

2.2.7 β-cylcodextrin/HDL Treatment and Stimulation of LXR Activity with T0901317

β-cylcodextrin stock solution (7.5 mM) and T0901317 stock solution (3 mM) were added to AM-F1-D1 for a final concentration of 0.75 mM and 3uM, respectively. Additionally, HDL was added to the same medium with a final concentration of 1 mg/mL, with the final volume at 12 mL. The treated media was added to 3T3-L1 cells on Day 5 of differentiation, made fresh, and changed daily, with 2mL of treatment solution per well. Treated 3T3-L1 cells were also monitored for lipid accumulation and viability.

2.3 RNA Isolation

Total RNA isolation from 3T3-L1 cells was performed using the TRIzol Reagent (Invitrogen), following the manufacturer protocol. 1 mL of TRIzol reagent was added to each well of the 6-well plates and incubated at room temperature for 10 min with shaking. Total contents of cells were transferred to 1.5 mL Eppendorf tubes and, if not processed immediately, stored at -80C. Phase separation was performed by adding 0.2 mL of choloroform per 1 mL of Trizol reagent in the homogenate. Samples were then shaken vigorously for 15 seconds and allowed to incubate at room temperature for 2 min. Subsequently, samples were centrifuged at 12,000 x g at 4C for 15 min, with the resulting RNA-containing supernatant transferred to clean RNase free tubes. RNA was then precipitated by adding 0.5 mL isopropanol per 1 mL of TRIzol reagent to the homogenate. Samples were shaken again for 15 min and incubated at room temperature for 10 min. Afterwards, samples were centrifuged again at 12,000 x g at 4C for 30 min to pellet the RNA. Upon removing the supernatant, precipitated RNA pellet was washed with 1 mL of 75% ethanol per 1 mL of TRIzol in the initial homogenate and air dried at room temperature for 5 min. RNA was re-suspended in 20 uL of RNA storage buffer (Ambion) and the concentration was determined using absorbance at 260 nm with a biophotometer (Beckman Industries).

Contaminating DNA was removed from the RNA using a DNA-free kit (Ambion) following the manufacturer protocol. Reaction mixtures typically contained 10 ug of RNA, 2 uL of 10X DNase I buffer, and 1 uL of DNase I and RNase-free water per 20 uL of reaction mixture. Samples were then gently mixed and incubated at 37C for 20-

30 min. To inactivate the DNase I, 5 uL of DNase I Inactivating Reagent was added to samples, followed by mixing and incubating samples at room temperature for 2 min. Samples were then centrifuged at 10,000 x g for 1 minute to pellet the inactivation reagent. Lastly, treated RNA samples were transferred to clean RNase-free tubes, and RNA concentration was determined using absorbance at 260 nm. Samples were stored at -20 for short- and long-term storage.

2.4 cDNA Synthesis

cDNA was synthesized from total RNA isolated by using the Omniscript Reverse Transcriptase Kit (Qiagen) following the manufacturer protocol. Reactions were run at 37C for 1 hour, and resulting cDNA samples were stored at -20C for short- and long-term storage.

2.5 Quantitative Real time PCR (QPCR)

Quantitative real time PCR was conducted using the fluorescent detection molecule SYBR Green (Applied Biosystems) and the manufacturer protocol. Individual reactions contained 5 uL (20 ng) of cDNA, 12.5 uL of 2X SYBR Green PCR Master Mix (Fisher Scientific), 5.5 uL of distilled, de-ionized water, and 1.0 uL each of 10 uM forward and reverse primers of desired gene tested (Table 2.1). Reaction mixtures were prepared in bulk and scaled up as necessary, including enough mixture for no template control (NTC) reaction wells. 5 uL of cDNA was first added to each well in a 96-well PCR reaction plate (Applied Biosystems) followed by 20 uL

of the reaction mixture, giving a total volume of 25 uL per reaction well. Subsequent reactions were run in the ABI Prism 700 Sequence Detection System (Applied Biosystems). PCR was initiated at 95C to activate the Taq DNA polymerase, followed by 45 cycles at 95C for 15 seconds and then at 60C for 1 minute. Dissociation analysis of PCR products was performed immediately following the last cycle of the program, using a 60 degree C to 95 degree C temperature range.

Table 2.1. Mouse Primers used in Quantitative Real-Time PCR (QPCR).

Mouse Gene	**Destination**	**Forward Primer**	**Reverse Primer**
TATA-Binding Protein	*Tbp*	ACCGTGAATCTTGGCTGTAAACTT	TCGCTTGGGATTATATTCAGCATT
Peroxisome proliferator-activated receptor, gamma	*Pparg*	TGGACCTCTCCGTGATGGAA	ATGCTGGAGAAATCAACTGTGGTA
Apolipoprotein C1	*ApoCI*	TCCTGTCCTGATTGTGGTCGT	CCAAAGTGTTCCCAAACTCCTT
Apolipoprotein E	*Apoe*	TGGGTGCAGACGCTTTCTG	TCAGTGCCGTCAGTTCTTGTG

2.6 Statistical Analysis

Quantitative PCR data was analyzed using ABI SDS Prism Software Version 1.0. Samples were obtained from triplicate cultures and triplicate PCR reactions were performed for each sample. Average CT values were first calculated, and then relative mRNA levels were determined using the $\Delta\Delta C_T$ method of relative quantitation, as described in the ABI User Bulletin #2 (Applied Biosystems, 1997) (. mRNA levels were calculated relative to the house-keeping reference gene TATA-box binding

protein (*Tbp*). Values obtained are means of the triplicate experiments +/- standard deviationStandard error for the samples was calculated using the following formula:

$$\text{Standard Error} = (\text{Standard deviation} / \sqrt{2})$$

and were appropriately averaged to reflect the triplicate experiments accordingly.

Table 2.2. The $\Delta\Delta C_T$ Method of Relative Quantitation of Gene Expression. Quantitative PCR data was analyzed by using the ABI $\Delta\Delta C_T$ method. Variable X denotes the day of differentiation, the Variable Target Gene denotes the gene of interest, and all results were normalized to the house-keeping gene, *Tbp*.

Calculated Value	Formula
$\Delta C_{T,\ \text{TARGET GENE}}$	Avg. $C_{T,}$ value for Day (X), $_{\text{TARGET GENE}}$ − Avg. $C_{T,}$ value for Day (X), $_{\text{REFERENCE GENE}}$
$\Delta C_{T,\ \text{CALIBRATOR}}$	Avg. $C_{T,}$ value for Day 0, $_{\text{TARGET GENE}}$ − Avg. $C_{T,}$ value for Day 0, $_{\text{REFERENCE GENE}}$
$\Delta\Delta C_T$	$\Delta C_{T,\ \text{CALIBRATOR}} - \Delta C_{T,\ \text{CALIBRATOR}}$
Fold Change	$2^{\wedge}(-\Delta\Delta C_T)$

2.7 Human Adipocytes Cell Culture Conditions

2.7.1 Human Adipocytes Culture Conditions for Supernatant Sample Collection

Human subcutaneous preadipocytes (ZenBio, Research Triangle Park, North Carolina) were commercially purchased and were originally isolated from the subcutaneous fat from the thigh of a healthy, non-diabetic 40-year-old female with a body mass index of 25.7. Cells were thawed in a 37C water bath for 2 min, and then 1 mL of vial volume was transferred to a 15 mL sterile conical tube. The tube was

centrifuged at 125 x g (1300 RPM) at 20C for 5 min. After centrifugation, cells were re-suspended in 10 mL of preadipocyte media (PM-1) (ZenBio) and with agitation. Additionally, while cells were being centrifuged, 17 mL of PM-1 was added to 3 T-75 flasks and left in the incubator at 37C and 5% CO2. To seed individual T-75 flasks, 3 mL of the re-suspended media was added to each T-75 flasks, bringing the total volume of the flask to 20 mL. Flasks were incubated at 37C at 5% CO2 and checked daily for viability. Cells were maintained by with PM-1, and media was changed every 48 hours.

Once cells reached 100% confluency from the initial seeding, cells were induced to differentiate using adipocyte differentiation medium (DM-2) (ZenBio) which was considered Day 0. Cells were washed 3 times with 1X PBS, and PM-1 was removed from the flask and replaced with DM-2

On Day 5, DM-2 was removed and replaced with insulin-free and dexamethasone-free adipocyte maintenance media (AM-FI-DI) (ZenBio) and changed according to the feeding volumes suggested by the supplier:

Table 2.3. Human Adipocyte Media Feeding Changes. Provided by ZenBio.

Format	Plating	Change PM-1 to DM-2		Change DM-2 to AM-1		Change AM-1 to AM-1	
	IN	OUT	IN	OUT	IN	OUT	IN
T-75 flask	20 ml/flask	20 ml/flask	20 ml/flask	12 ml/flask	16 ml/flask	12 ml/flask	12 ml/flask

2.7.2 Human Adipocytes Used in Immunofluorescence Imaging

Human subcutaneous preadipocytes (ZenBio) were passaged cells (passage 30) from previous cells originally isolated from the subcutaneous fat from the thigh of a healthy, non-diabetic 40-year-old female with a body mass index of 25.7. Cells were thawed in a 37C water bath for 2 min and then transferred to a 15 mL sterile conical tube with 9 mL of preadipocyte media (PM-1) (ZenBio). The tube was centrifuged at 125 x g (1300 RPM) at 20C for 5 min. During centrifugation, 2 mL of PM-1 was added to one T-25 flask and left in the incubator at 37C and 5% CO2. Directly following centrifugation, cells were re-suspended in 3 mL of PM-1, with agitation, and added directly onto the previously mentioned T-25 flask, bringing the total flask volume to 5 mL. The flask was incubated at 37C at 5% CO2 and checked daily for viability. Cells were maintained by with PM-1, and media was changed every 48 hours.

Once cells reached 70% confluency from the initial seeding, cells were split once more and seeded onto flame-sterilized glass cover slips (Fisher Scientific) in 6-well plates. To split the T-25 flask, cells were first washed 3 times with PBS. After washing, 0.5 mL of Trypsin/EDTA was added to the flask and incubated for 5 min. Once 80% of cells were lifted from the flask bottom, 5 mL of PM-1 was added to the T-25 flask. The total cell suspension was then transferred to a 15 mL centrifuge tube and centrifuged at 125 x g for 5 min. After centrifugation, the media was decanted leaving the pellet, and the cell pellet was resuspended in 4 mL of PM-1. Cells were counted using the Trypan Blue Staining protocol and added to individual wells of 6-

well plates containing flame-sterilized glass cover slips. Final cell density was 50,000 cells per well in 2 mL of PM-1. Cells were maintained by with PM-1, and media was changed every 48 hours.

When cells reached 50% confluency per well, adipocyte differentiation was induced using purchased adipocyte differentiation medium (DM-2) (ZenBio); the day of differentiation was then designated as Day 0. Cells were washed 3 times with 1X PBS, and PM-1 was removed from the flask and replaced with DM-2.

On Day 5, DM-2 was removed and replaced with insulin-free and dexamethasone-free adipocyte maintenance media (AM-FI-DI) (ZenBio) and changed according to the feeding volumes suggested by the supplier (Table 2.2).

2.7.3 Trypan Blue Staining

Trypan Blue staining was conducted to determine cell viability and subsequent cell suspension volumes necessary to seed at 50,000 cells per glass cover slip. After washing cells in the centirufgation step following trypsinization, 100 uL of the 4mL cell suspension was added to 100 uL of Trypan Blue working solution (Invitrogen) in a 1.5 mL Eppendorf tube. The solution was mixed well, and 10 uL was loaded onto a hemocytometer (Cascade Biologies) to access viable (non-dyed) and non-viable (blue-dyed) cells using phase-contrast microscopy.

2.8 Supernatant Collection and Sample Ultracentrifugation

Differentiated human subcutaneous adipocyte supernatant samples were collected on Days 0, 7, 11, and 14 (D0, D7, D11, and D14) during the July 2007 time course and Days 0, 9, 11, and 13 (D0, D9, D11, and D13) during the July 2008 time course of the experiment. Day 0 signified the first day of differentiation induction, while Days 7 and 9 were used as time-points for late-phase human adipocyte differentiation. Days 11 and 13 were time-points for fully mature human adipocytes, as described in the ZenBio cell culturing manual (Figure 1.4. Before changing media, supernatants were collected in sterile 1.5 mL Eppendorf tubes, labeled, and stored in -80C for long term storage and -20C for short term storage.

3T3-L1 supernatant samples were collected in the same manner on Days 0, 3, 6 and 9 (D0, D3, D6, and D9) for stimulated and treated cells during the July 2008 time course of the experiment. Samples were also stored in the same manner.

To prepare the samples for ultracentrifugation, supernatant samples were brought to a density of 1.21 g/mL using NaBr and centrifuged at 50,000 RPM at 15C for 43 hrs in the Beckman Ti60 rotor. Fractions were collected throughout the heat-sealed tube by inserting a 20cc gage needle and dripping sample layers into labeled 1.5 mL Eppendorf tubes. Using a Fisher Scientific Multidialysis system, fraction samples were dialyzed twice against 1X PBS (10 mM PBS, pH 7.4) at 4 degrees C overnight.

2.9 SDS-PAGE

Samples were prepared with 2x reducing sample buffer (0.125M Tris-HCL, 0.1% SDS, 4% SDS, 20% glycerol, 5 mg of DTT per 1 mL sample buffer, pH6.8) with final protein concentration at 1ug/mL. Samples were then heated in an 80C water bath for 15 min. Afterwards, samples were loaded onto 5-25% acrylamide gradient gels with 20 uL of sample per well. Gels electrophoresis was conducted for 40 min at 35 mA per gel using the Fisher Scientific Vertical Electrophoresis Systems 10x10cm®. Once desired separation was achieved, gels were either stained with Coomasie Blue stain or blotted onto nitrocellulose membrane.

2.9.1 Coomassie Blue Staining

Gels were stained with Coomassie Blue stain solution (0.025% Coomassie Blue R-250, 40% methanol, 7% acetic acid) at room temperature for 2-4 hours while shaking. Stain was then decanted and replaced with Destaining solution I (50% methanol, 10% acetic acid). After incubating with Destaining solution I while shaking, the solution was also decanted and replaced with Destaining solution II (5% methanol, 10% acetic acid) for 1 hour. Afterwards, gels were visualized using FluorChem 800 imager.

2.9.2 Western Blot Analysis

Gels were blotted onto nitrocellulose membrane using the Fisher Scientific Mini-tank Electroblotter® for 30 min at 100 mA per blot. Afterwards, nitrocellulose membranes were blocked with TBS-5% milk for one hour at 4C. Membranes were

then incubated with commercially-purchased goat anti-human APOC-I IgG (K74120G, BioDesign International, Saco, Maine) conjugated with horseradish peroxidase (HRP) at a concentration of 1:1000 overnight at 4C. Blots were then developed using AlphaInnotech® Chemiluminescent Western blot reagents (Alpha Innotech Corporation, San Leandro, California) at 0.125 mL reagent per cm^2 of nitrocellulose membrane.

2.10 Slot Blot Assay

The Minifold II apparatus (Schleicher & Schuell, Keene, NH) containing the base section, the red silicone spacer, and vacuum filter support section was first assembled following the manufacturer protocol. One Schleicher & Schuell GB002-SB filter paper was pre-wet in 1X PBS solution and placed on top of the vacuum section support. One S&S nitrocellulose membrane was pre-wet in 1X PBS and placed onto the bottom side of the upper sample well plate, and the surface was smoothed to ensure no bubbles were trapped between the layers. The upper sample well plate with the nitrocellulose was then placed on top of the vacuum section support with filter paper. The Minifold apparatus was clamped firmly and subsequently vacuumed to seal layers.

After vacuum sealing, samples were loaded into individual wells and then vacuumed through. Once samples were vacuumed through, Minifold apparatus was unclamped and nitrocellulose paper was washed with 30 mL of distilled, de-ionized water twice. To detect desired antigen(s) in the sample, nitrocellulose was first blocked with 1X TBS-5% milk solution at 4C for 1 hr with rocking. The desired

primary antibody was added to the TBS-5% milk solution, and the nitrocellulose was left rocking at 4C overnight. Following primary antibody incubation, nitrocellulose membranes were washed 3 times with 50 mL of 1X TBS at room temperature for 5 min each wash and rocking. Membranes were then incubated with appropriate secondary antibodies in TBS-5% milk at room temperature for 1 hour. Membranes were again washed 3 times with 50 mL of 1X TBS for 5 min and rocking each wash. Lastly, membranes were either developed using a chromogenic substrate solution 4-chloro-1-napthol (4CN) in methanol, TBS, and H_20_2 or AlphaInnotech® Chemiluminescent Western blot reagents at 0.125 mL reagent per cm^2 of nitrocellulose membrane. Imaging was done using the FluorChem 800 imaging system.

2.11 Immunofluorescence

Human adipocytes grown to 50% confluency on glass cover slips (gift of Dr. Gary Laverty, University of Delaware) in 6-well plates were immunostained using a combination of commercially-purchased rabbit anti-human APOC-I (K74110R, BioDesign International, Saco, Maine) and goat a-rabbit FITC conjugated IgG (a generous gift of Aravindand Rolands, DeLeon Laboratory, University of Dealware).

2.11.1 Stimulated Human Adipocyte Immunostaining Conditions

Media was first removed from individual wells, labeled and stored in 15 mL centrifuge tubes. Cover slips were then washed twice with warm, sterile 1X PBS and

fixed with 3.7% paraformaldehyde in PBS at room temperature. After fixation, cover slips were washed twice again with 1X PBS and blocked with a 2% BSA-PBS solution for 10 min at 37 degrees Celsius. The cover slips were then incubated in a humid chamber at 37 degrees C for 45 min in an anti-APOC-I antibody solution made with 2% BSA-PBS to a dilution of 1:100 of the antibody (rabbit IgG, K74110R, BioDesign International). Following incubation, cover slips were washed three times in PBS and incubated with FITC-conjugated anti-rabbit IgG in a 1:100 dilution in 2% BSA-PBS for 30 min in a humidifying chamber at 37 degrees C. Cover slips were washed once three times more after incubation and mounted with a 1:1 (vol/vol) solution of glycerol and PBS onto glass slides.Visualization was conducted using Zeiss Axioskop microscope and the Kodak MD 290 Imaging System.

2.11.2 Heparinase-Treated Human Adipocyte Immunostaining Conditions

Media was first removed from individual wells, labeled and stored in 15 mL centrifuge tubes. Cover slip were then washed twice with warm, sterile 1X PBS and incubated with heparinase (3 units/ mL, generous gift of Brian Danysh, Duncan Lab, University of Delaware) in 1 mL of AM-F1-DI media for 2 hours in humidifying chamber at 37 degrees C (Burgess, Gould, & Marcel, 1998). Afterwards, media was removed and stored in labeled 1.5 mL Eppendorf tubes. Cover slips were then washed twice with warm 1X PBS and fixed with 3.7% paraformaldehyde in PBS at room temperature. After fixation, cover slips were washed twice again with 1X PBS and blocked with a 2% BSA-PBS solution for 10 min at 37 degrees Celsius. The cover

slips were then incubated in a humid chamber at 37 degrees C for 45 min in an anti-APOC-I antibody solution made with 2% BSA-PBS to a dilution of 1:100 of the antibody (rabbit IgG, BioDesign International). Following incubation, cover slips were washed three times in PBS and incubated with FITC-conjugated anti-rabbit IgG in a 1:100 dilution in 2% BSA-PBS for 30 min in a humidifying chamber at 37 degrees C. Cover slip were washed once three times more after incubation and mounted with a 1:1 (vol/vol) solution of glycerol and PBS onto glass slides.Visualization was conducted using Zeiss Axioskop microscope and a Kodak MD 290 Imaging System.

2.11.3 Heparinase-Treated and Permeabilized Human Adipocyte Immunostaining Conditions

Media was first removed from individual wells, labeled and stored in 15 mL centrifuge tubes. Cover slips were then washed twice with warm, sterile 1X PBS and incubated with heparinase (3 units/ mL) in 1 mL of AM-F1-DI media for 2 hours in humidifying chamber at 37 degrees C. Afterwards, media was removed and stored in labeled 1.5 mL Eppendorf tubes. Cover slips were then washed twice with warm 1X PBS and fixed with 3.7% paraformaldehyde in PBS at room temperature. After fixation, cells were permeabilized by incubating with 0.5% Triton-X 100 in PBS for 5 min at 37 degrees C (Ji, Brecht, Miranda, Hussain, Innerarity, & Mahley, 1993). Cover slips were then blocked with a 2% BSA-PBS solution for 10 min at 37 degrees Celsius. The cover slips were then incubated in a humid chamber at 37 degrees C for 45 min in an anti-APOC-I antibody solution made with 2% BSA-PBS to a dilution of

1:100 of the antibody (rabbit IgG, BioDesign International). Following incubation, cover slips were washed three times in PBS and incubated with FITC-conjugated anti-rabbit IgG in a 1:100 dilution in 2% BSA-PBS for 30 min in a humidifying chamber at 37 degrees C. Cover slips were washed once three times more after incubation and mounted with a 1:1 (vol/vol) solution of glycerol and PBS onto glass slides.Visualization was conducted using Zeiss Axioskop microscope and a Kodak MD 290 Imaging System.

2.11.4 Stimulated and Treated Human Adipocyte Control Immunostaining Conditions

Cells were treated and stained as aforementioned in either stimulated or treated conditions. However, instead of incubating cover slips in rabbit anti-human APOC-Isolution, cover slips were incubated in 2% BSA-PBS solution for 45 min in humidifying chambers at 37 degrees C for blocking. Afterwards, cover slips were incubated in 1:100 of antibody in 2% BSA-PBS (vol/vol) of FITC-conjugated goat anti-rabbit IgG for 30 min in a humidifying chamber at 37 degrees C.

Chapter 3

RESULTS

3.1 Expression of Gene Markers during 3T3-L1 Adipocyte Differentiation

Using the mouse 3T3-L1 pre-adipocyte cell line, adipocyte differentiation can be induced using an established differentiation protocol and confirmed either by determining the ratio of cells with lipid droplets to those without or by QPCR using an internal controls, adipsin and TBP. Ratios of expression should exceed 10:1 for good induction of differentiation. Markers for early, intermediate, and late gene activation are SREBP-1, PPARγ and adipsin, respectively. Upon reaching confluency, 3T3-L1 pre-adipocytes are growth arrested and induced to differentiation to adipocytes. Key events of 3T3-L1 pre-adipocyte differentiation include the commencement of early gene activation and DNA replication followed by activation of intermediate genes (Figure 1.3). The induction of intermediate genes, usually transcription factors expressed between Days 1 to 3, leads to the stimulation of late genes involved in further growth arrest and lipid droplet biogenesis in subsequent days.

First, all QPCR values were normalized to mRNA expression of the housekeeping gene TATA-binding protein (*Tbp*) in 3T3-L1 cell lines. The TBP protein is the constitutively expressed component of the transcription factor TFIID which ultimately

acts as the RNA pol II pre-initiation complex important in gene transcription. *Tbp* mRNA expression was constant during 3T3-L1 differentiation and remained unaffected by various experimental treatments, which proves pivotal for an ideal reference gene (Figure 3.1). *Tbp* expression varied less than one-fold throughout the differentiation time course.

To verify that the 3T3-L1 pre-adipocyte cell line underwent proper differentiation, quantitative real-time PCR was conducted for the previously established intermediate gene peroxisome proliferator-activated receptor gamma (PPARγ) and normalized to the internal reference gene *Tbp*. PPARγ is a nuclear receptor protein which dimerizes with retinoid-X-receptor and acts as a transcription factor for genes involved in lipid uptake and adipogenesis, in short late genes. The Usher lab determined in prior studies that PPARγ mRNA expression in 3T3-L1 cells is first expressed on Day 1, exhibits a 8- to 10-fold increase by Day 3, and reaches a maximum of 15-fold on Day 6. (unpublished, David, 2006). In this study, there was only a 1-fold increase on Day 3 and a 4-fold increase on Day 6 (Figure 3.2), indicating that differentiation was either poor or that the primers were degraded. QPCR results, however, conflicted with the numerous lipid droplets observed in Day 6 mouse 3T3-L1. Thus, while the values differ from the previous study possibly because of poor reagents, the *Pparγ* expression pattern is the same.

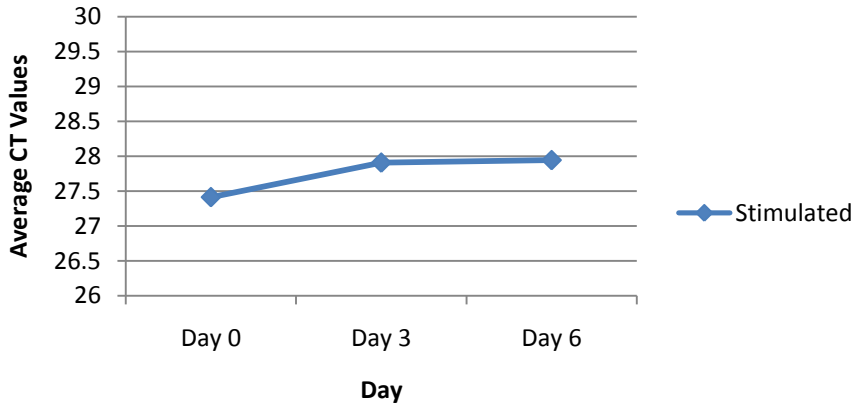

Figure 3.1. Average CT Values for *Tbp* mRNA Expression.Stimulation of Tbp was performed at Day 0 using DM-1 media and maintained from Day 5 on with AM-FI-FD media for a time-course of 9 days. Quantitative RT-PCR was performed using RNA isolated from 3T3-L1 Day 0, 3, and 6 adipocytes.

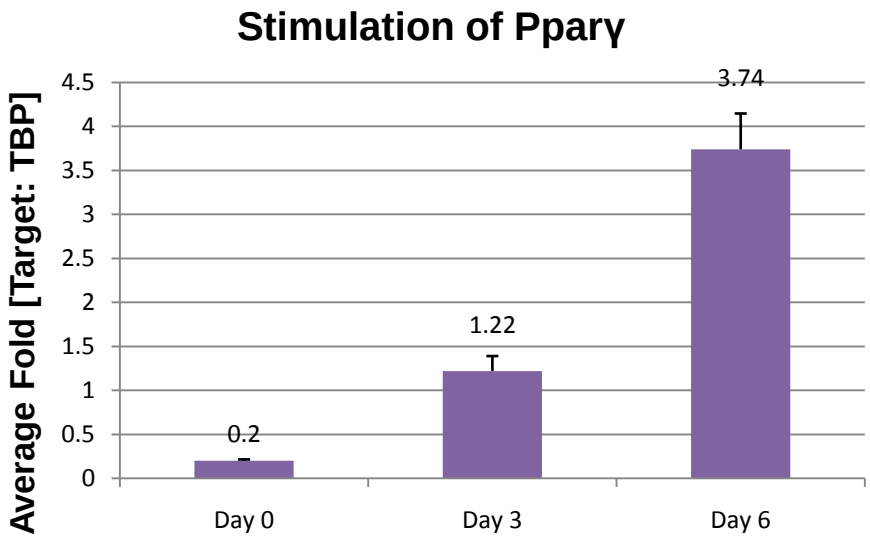

Figure 3.2. Stimulation of Mouse *Pparγ* mRNA during Adipocyte Differentiation. Stimulation of Pparγ was performed at Day 0 using DM-1 media and maintained from Day 5 on with AM-FI-FD media for a time-course of 6 days. Quantitative RT-PCR was performed using RNA isolated from 3T3-L1 Day 0, 3, and 6 adipocytes. Relative mRNA levels and subsequent average fold values were normalized to the reference gene *Tbp*.

3.2 Apoliproteins E and C-I mRNA Expression in 3T3-L1 Adipocytes

Apoe mRNA expression in differentiated mouse 3T3-L1 cells peaked at Day 3, showing a 4.01-fold increase over *Tbp* mRNA expression (Figure 3.3). Though this shows a similar fold-increase in 3T3-L1 cells previously established by the Usher lab, *Apoe* mRNA expression did not remain the same for the remaining days, and instead dropped to a 1.86-fold increase by Day 6 (unpublished, David, 2006; unpublished, Sterling, 2007).

Unlike *Apoe* mRNA expression, *Apoc1* increased as differentiation progressed. Again, *Apoc1* mRNA expression was normalized to *Tbp*, and like previous data

established by the Usher lab, *Apoc1* mRNA showed the highest expression on Day 6 during late-phase differentiation (Figure 3.3.). On Day 3, or intermediate-gene expression, *Apoc1* mRNA increased about double from 0.04-fold to 0.69-fold, and finally increased to 1.86-fold on Day 6. Compared to previous values established by the Usher Lab, this is between 20- and 40-fold lower and may either be a function of poor stimulation or poor primers. Regardless, the pattern of expression is similar to what was found before, that *Apoc1* mRNA is expressed most during late differentiation.

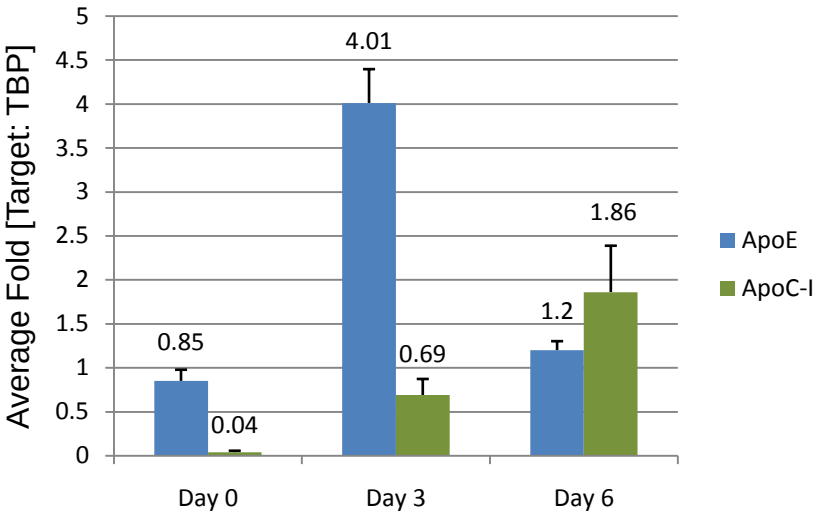

Figure 3.3. Relative Expression of Stimulated *Apoe* and *Apoc1*. Stimulation of apoE and apoC-I was performed at Day 0 using DM-1 media and maintained from Day 5 on with AM-FI-FD media for a time-course of 9 days. Quantitative RT-PCR was performed using RNA isolated from 3T3-L1 Day 0, 3, and 6 adipocytes. Relative mRNA levels were normalized to the reference gene *Tbp*.

3.3 Apolipoproteins E and C-I mRNA Expression in Treated 3T3-L1 Adipocytes

3.3.1 Changes in Apolipoprotein E mRNA Expression in Treated 3T3-L1 Adipocytes

A serum-free media treatment was used to elucidate the effects of extracellular lipoprotein acceptors on *Apoe* mRNA expression. Since the serum-free media was devoid of lipoproteins typically found in fetal bovine serum, a constituent of serum-enriched adipocyte media, *Apoe* mRNA expression was detected on Day 6 in mouse 3T3-L1 adipocytes. *Apoe* mRNA levels about doubled, increasing from 1.2-fold in stimulated cells to 2.83-fold in serum-free treated cells (Figure 3.4).

The second treatment with Intralipid, a commercially-purchased lipid emulsification, was added to serum-free media to act as a lipoprotein cholesterol-acceptor, albeit without the proteins normally associated with extracellular lipoproteins, and a potential stimulant of cholesterol efflux genes. Similar to the effects of normal serum-free media, the Intralipid treatment increased *Apoe* mRNA from 1.2-fold observed in the stimulated control to 2.19-fold observed in the treated cells (Figure 3.4).

The Liver-X-Receptor ligand agonist, T0901317, is an oxysterol derivative known to induce LXR production in mammalian cells. It enables LXR dimerization with retinoid-X-receptor, a similar transcription factor, wherein both translocate to the nucleus and activate various cholesterol efflux genes. Since LXR/RXR stimulates

cholesterol efflux genes, the LXR agonist addition serves to demonstrate the effects on a well-established cholesterol efflux protein ApoE and on the potential cholesterol efflux protein apoC-I. Similar to previous studies conducted by the Usher lab, *Apoe* mRNA expression was upregulated about 4-fold, which is about triple the mRNA expression in stimulated cells (Figure 3.4)

Incubation with β-cylcodextrin, a cyclic oligosaccharide which sequesters cholesterol, and exogenous HDL particles which act as a cholesterol sink allowed for cholesterol depletion of 3T3-L1 adipocytes, showed a significant decrease in *Apoe* mRNA expression. *Apoe* mRNA levels decreased slightly from 1.2-fold in stimulated cells to 0.99-fold in treated cells which was not a significant drop as observed in previous studies (Figure 3.4).

The combined treatment of LXR stimulation by T0901317 and cholesterol depletion with β-cylcodextrin and HDL incubation yielded varied results. *Apoe* mRNA levels increased in comparison with LXR agonist alone, which disagreed with previous studies using the combined LXR and β-cylcodextrin treatments. This may be because the β-cylcodextrin treatment, which has been previously shown to significantly lower *Apoe* expression, was not as effective in cholesterol depleting cells in this study.

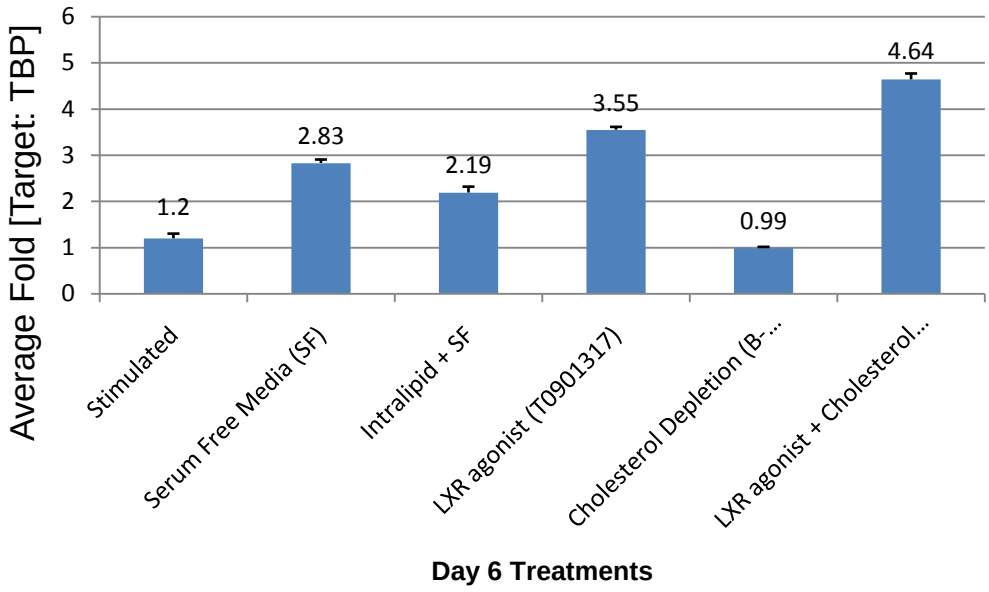

Figure 3.4. Average Fold *Apoe* mRNA Expression in Treated 3T3-L1 Adipocytes. Stimulation of *Apoe* was performed at Day 0 using DM-1 media and maintained from Day 5 on with AM-FI-FD media for a time-course of 9 days. Treatments began on Day 5 with serum-free media, Intralipid and serum-free media, LXR agonist T0901317 in AM-FI-FD media, β-cyclodextrin, HDL and AM-FI-FD media, and a combined treatment of LXR agonist T0901317, β-cyclodextrin, HDL and AM-FI-FD media. Treatments were changed daily. Quantitative RT-PCR was performed using RNA isolated from 3T3-L1 Day 6 adipocytes. Relative mRNA levels were represented as average fold values relative to the reference gene *Tbp*.

3.3.2 Changes in Apolipoprotein C-I mRNA Expression in Treated 3T3-L1 Adipocytes

Similar to the increased *Apoe* mRNA expression after serum-free treatments, *Apoc1* also exhibited a three-fold increase compared to the stimulated control (Figure 3.5). *Apoc1* mRNA expression increased from 1.86-fold in stimulated cells to 6.76-fold in treated cells (Figure 3.5).

Moreover, in the Intralipid-treated cells *Apoc1* mRNA expression was increased as well and at levels much higher than *Apoe* mRNA levels (Figure 3.5). For instance, *Apoc1* mRNA expression rose from 1.86-fold in stimulated, control cells to 5.67-fold in treated cells, which was about 1.5 times more than *Apoe* expression (Figure 3.4).

LXR agonist T0901317 treatment increased *Apoc1* mRNA expression, like*Apoe* mRNA expression. *Apoc1* mRNA expression increased from 1.86-fold in stimulated cells to about 6.71-fold-fold in treated cells(Figure 3.5); interestingly, *apoc1* mRNA levels were much greater than relative levels of *Apoe* expression since *Apoe* mRNA expression was at 0.88 (Figure 3.4).

In cholesterol depleted cells *Apoc1* mRNA levels also decreased, dropping from 1.86-fold in stimulated cells to 0.46-fold, about a four-fold decrease (Figure 3.5). Additionally, *Apoc1* mRNA expression exhibited the varied outcome seen with *Apoe* expression in cells treated with both LXR agonist and cholesterol depletion. In co-treated cells *Apoc1* mRNA expression was at 24-fold, which was more than cholesterol depletion alone (0.46-fold) and the stimulated control (1.86-fold) which was expected, but it was also much higher than LXR agonist (6.71-fold). Since combined LXR agonist and cholesterol depletion was higher than LXR agonist, when it should have been lower, the reason may be because of ineffective cholesterol depletion (Figure 3.5).

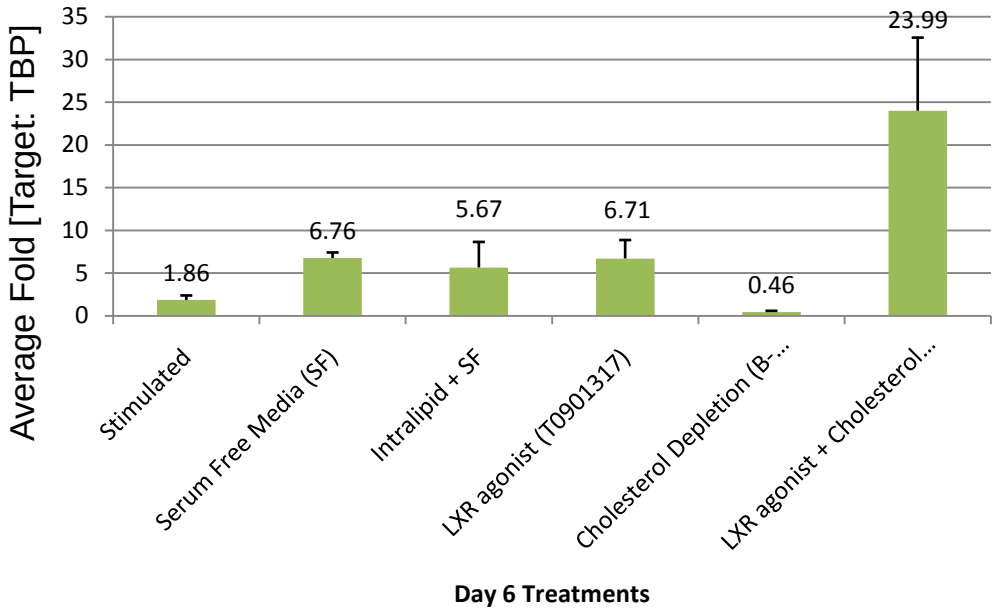

Figure 3.5. Average Fold *Apoc1*mRNA Expression in Treated 3T3-L1 Adipocytes. Stimulation of *Apoc1* was performed at Day 0 using DM-1 media and maintained from Day 5 on with AM-FI-FD media for a time-course of 9 days. Treatments began on Day 5 with serum-free media, Intralipid and serum-free media, LXR agonist T0901317 in AM-FI-FD media, β-cyclodextrin, HDL and AM-FI-FD media, and a combined treatment of LXR agonist T0901317, β-cyclodextrin, HDL and AM-FI-FD media. Treatments were changed daily. Quantitative RT-PCR was performed using RNA isolated from 3T3-L1 Day 6 adipocytes. Relative mRNA levels were represented as average fold values relative to the reference gene *Tbp*.

3.4 Apolipoprotein C-I Detection in Human Adipocyte Supernatant

3.4.1 Apoliporotein C-I Production in Isolated Fractions from Human Adipocyte Supernatants

To determine APOC-I association with lipoprotein fractions, supernatants were collected from stimulated Day 13 human subcutaneous adipocytes. Next, supertantant samples were then density-adjusted to 1.21 g/mL which, during ultracentrifugation (described in the methods), allows the lipoprotein fraction to float to the top. After

ultracentrifugation, 23 fractions from the top of the centrifuge tube to the bottom were collected (described in the methods). The fractions were then visualized for APOC-I using goat anti-human APOC-I (Figure 3.13). Results indicated that bottom-most and top-most fractions contained the most APOC-I. This indicates that APOC-I may be associated with lipoproteins found in the top fraction but is also present in a lipid free state.

Although the additional positive control of purified human APOC-I was not visualized in the slot blot, this may be because the purified human APOC-I used in the assay was old and from 2003. New purified human APOC-I was purchased in 2008 and used for the remaining blots.

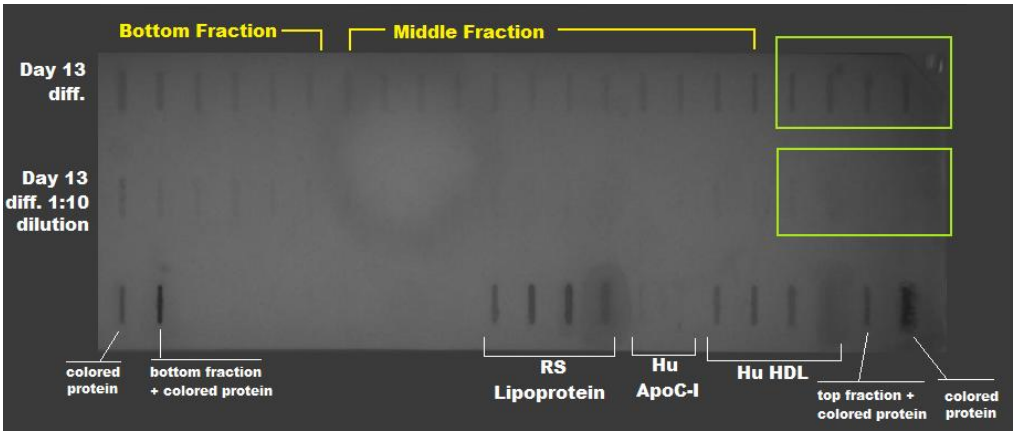

Figure 3.6. Immunoslotblot of 1 and 1:10 Dilution of Day 13 Differentiated Supernatant Fractions. Supernatant collected from Day 13 human adipocytes were density-adjusted to 1.21 g/mL, centrifuged, but not dialyzed. Green box denotes lipoprotein fraction containing HDLs. Human whole (RS) lipoprotein (1:100 serial dilution), human HDL (1:1000 serial dilution), and purified human APOC-I (1:10 dilution) was used as positive controls.

3.4.2 Apoliporotein C-I Production in Lipoprotein Fractions during Human Adipocyte Differentiation

The time-dependent production of APOC-I in the lipoprotein (top) fraction of supernatant samples was tested for supernatants collected on Days 0, 7, 9, 11, and 13 (Figure 3.7). The western blots could not detect APOC-I in any of the supernatant samples, though samples were loaded at 1ug/mL concentrations. Previous research has determined that APOC-I mRNA levels are highly upregulated late in human adipocyte differentiation and peaks at Day 8 (unpublished, Sara Sterling, 2007), thus it was expected that APOC-I protein expression would mirror mRNA levels. However, research has also shown that APOC-I is found at extremely low concentrations in the plasma: 4-7 mg/dL in contrast to 90-130 mg/dL for APOA-I, indicating that APOC-I production in supernatant samples may be too little for western blot detection (Cohn, et al., 2003). Thus, immunoprecipitation with polyclonal purified APOC-I antibodies, a method concentrating protein in samples, would best verify western blot results.

Figure 3.7. APOC-I Production in Top (Lipoprotein) Fractions. Supernatant samples collected from differentiated Days 0, 7, 9, 11, and 13 human adipocytes. Top fractions of each supernatant sample was combined with 10 μL 2X reducing sample buffer and heated for 15 minutes at 80 degrees C. Samples were run at 35 mA/gel for

(continued) 40 minutes and blotted onto nitrocellulose at 100 mA/gel for 30 min. Horseradish peroxidase-conjuaged goat anti-human APOC-I IgG (1:1000) used as detecting antibody, and samples were visualized using chemiluminescence.

3.5 Apolipoprotein C-I Detection on the Human Adipocyte Surface

To test whether APOC-I associates with the adipocyte surface, the 3-D APOC-I protein structure was first visualized to determine potential HSPG binding regions. Using the NCBI database, the APOC-I protein structure revealed 12 potential lysine and arginine binding sites (22% of total amino acid sequences) to heparan sulfate (Figure 3.8) and 16 hydrophic amino acids, or potential cholesterol-binding sites, which is 29% of total amino acids (Figure 3.9).

Once potential HSPG binding was confirmed, human adipocytes were grown on glass cover slips, induced to differentiate, and imaged using phase-contrast and immunofluorescence microscopy. Differentiation was used induced prior to reaching complete confluency since imaging cell borders would be easier at a lower cell density. Both the human subcutaneous preadipocyte and Day 0 adipocyte exhibited the canonical cellular morphology: cells were fibroblast-like, with thin, elongated cellular processes (Figure 3.10a). Moreover, by Day 6, the accepted period of lipid accumulation and cellular differentiation, phase contrast imaging revealed that the human adipocytes displayed a more cuboidal shape with intracellular lipid droplet formation (Figure 3.12a, b). Human adipocytes imaged on Day 10 revealed the accepted differentiated adipocyte morphology with much smaller, though with numerous lipid droplets (Figure 3.13a).

After phase-contrast imaging, epi-fluorescence microscopy was utilized to image cells after fixation and incubation with rabbit anti-human APOC-I antibodies and goat anti-rabbit FITC-conjugated secondary antibodies. For human subcutaneous preadipocytes and Day 0 adipocytes, there were no detectable fluorescent images (Figure 3.10b). Additionally, on Day 3 immunofluorescent images taken at 20X and 40X objectives revealed a faint, diffuse pattern, indicative of background from the FITC-conjugated secondary antibody (Figure 3.11b). Meanwhile the control, which was Day 3 human adipocytes blocked in 2% BSA-PBS and incubated with only FITC-conjugated secondary antibody, exhibited a similar diffuse stain but to a lesser extent (Figure 3.11a).However, on Day 6 APOC-I detection was confirmed when stimulated cells incubated with both primary and secondary antibodies exhibited a distinct fluorescent pattern; APOC-I protein clusters were dispersed on the adipocyte surface in a clear, punctate pattern (Figure 3.12c, d, e). Meanwhile the Day 6 control, which was human adipocytes incubated in only blocking solution and secondary antibody, exhibited the same diffuse pattern reminiscent of Day 3 immunofluorscent images (Figure 3.11a, Figure 3.12f). This demonstrated that protein visualization was not because of non-specific secondary antibody binding. Lastly, immunofluorescent images captured on Day 10 revealed the same punctate pattern of APOC-I proteins on the cellular surface, with the control exhibiting the familiar diffuse pattern from Days 6 and 3 (Figure 3.13b).

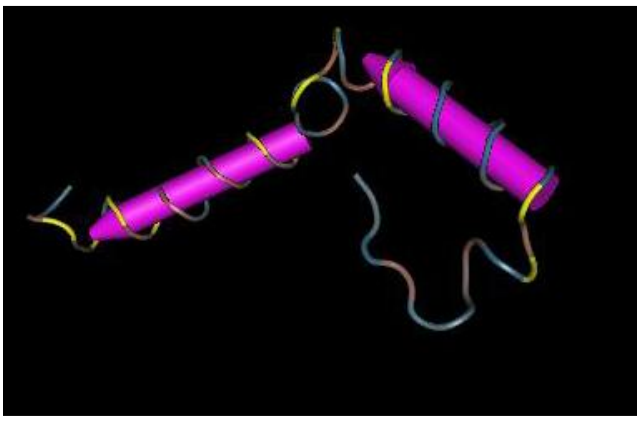

Figure 3.8. APOC-I Lysine and Arginine Residues. Lysine (K) and arginine (R) residues highlighted in yellow.

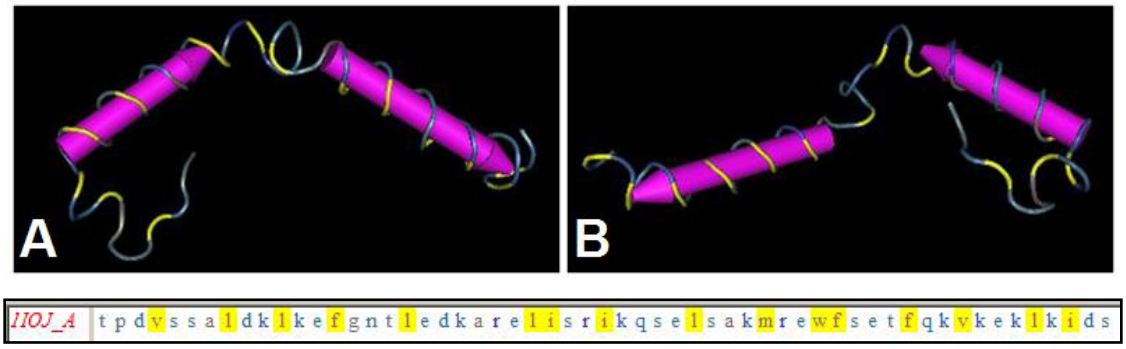

Figure 3.9. APOC-I Hydrophobic Regions and Correlating Amino Acid Residues. (A) Frontal view of APOC-I (B) Rotated 180 degree View. Hydrophobic regions highlighted in yellow on protein structure with correlating amino acid residue highlighted in protein sequence. Note amphipathic nature of APOC-I alpha helices.

Figure 3.10. Stimulated Day 0 Human Adipocyte. Stimulated Day 0 human adipocytes grown on glass cover slips. After fixation, blocking, and washing, cells were incubated with rabbit anti-human APOC-I IgG (1:100) for 45 min at 37 degrees C, washed, and then incubated with fluorecein isothiocyanate conjugated goat anti-rabbit IgG (1:100) for 30 min at 37 degrees C. (A) Phase-contrast image of Day 0 stimulated human adipocyte at 20X. (B) Immunofluorescent image with fluorescein filter of Day 0 stimulated cells. (C) Day 0 Adipocyte control. Cells were incubated with only FITC-conjugated goat anti-rabbit IgG (1:100). All images taken with Zeiss Axioskop and Kodak MDS 290 imaging system at 20X objectives. All bars equal 50 μm.

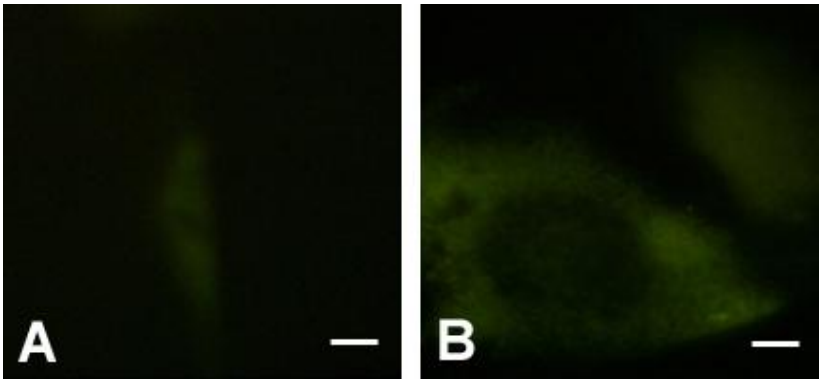

Figure 3.11. Stimulated Day 3 Human Adipocyte. Stimulated Day 3 human adipocytes grown on glass cover slips. After fixation, blocking, and washing, cells were incubated with rabbit anti-human APOC-I IgG (1:100) for 45 min at 37 degrees C, washed, and then incubated with fluorecein isothiocyanate conjugated goat anti-rabbit IgG (1:100) for 30 min at 37 degrees C. (A) Day 3 human adipocyte control. Cells were blocked in 5% BSA-PBS for 45 min and incubated with FITC-conjugated goat anti-rabbit IgG (1:100) for 30 min at 37 degree C. (B) Day 3 stimulated human adipocytes. All images taken on immunofluorescent fluorescein filter on Zeiss Axioskop and Kodak MDS 290 imaging system at 20X objective for 2.0 seconds. All bars equal 50 μm.

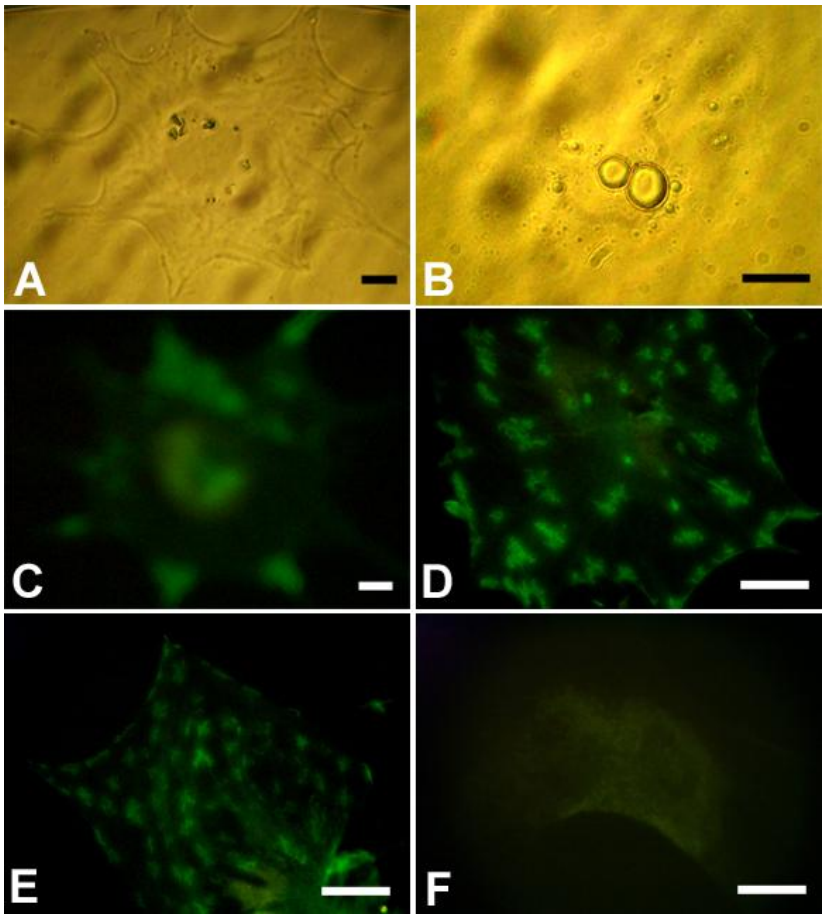

Figure 3.12. Stimulated Day 6 Human Adipocytes. Stimulated Day 6 human adipocytes grown on glass cover slips. After fixation, blocking, and washing, cells were incubated with rabbit anti-human APOC-I IgG (1:100) for 45 min at 37 degrees C, washed, and then incubated with FITC-conjugated goat anti-rabbit IgG (1:100) for 30 min at 37 degrees C. (A) Day 6 stimulated human adipocyte. Phase contrast image taken at 20X objective. (B) Lipid droplets from Day 6 stimulated human adipocytes visualized with phase-contrast microscopy at 40X objective. (C) Day 6 stimulated human adipocyte from *(A).* Fluorescein filter used with 20X objective, exposed for 2.0 seconds. (D) and (E) are Day 6 stimulated human adipocytes with punctuate APOC-I pattern. Imaged using immunofluorescent FITC-filter at 40X objective. (F) Stimulated Day 6 human adipocyte control, incubated with only FITC-conjugated goat anti-rabbit antibody (1:100). All bars equal 50 μm.

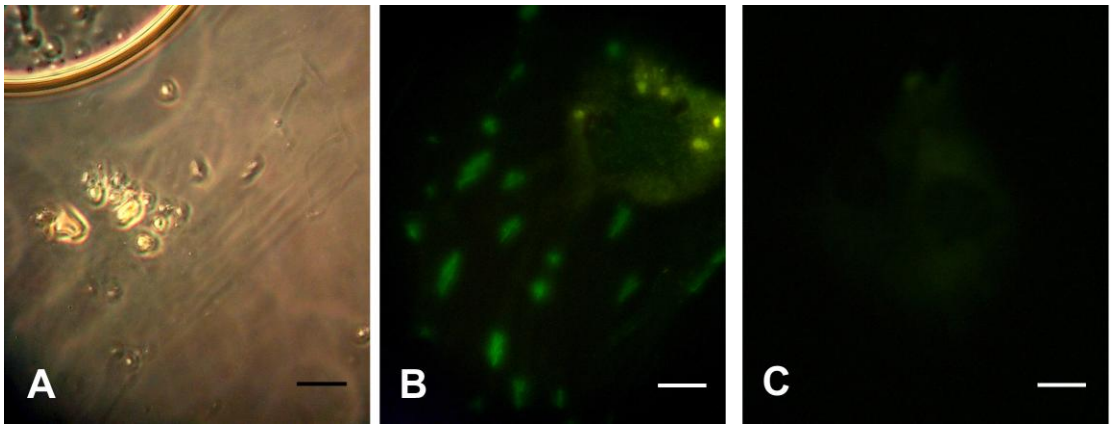

Figure 3.13. Stimulated Day 10 Human Adipocytes. Stimulated Day 10 human adipocytes grown on glass cover slips. After fixation, blocking, and washing, cells were incubated with rabbit anti-human APOC-I IgG (1:100) for 45 min at 37 degrees C, washed, and then incubated with FITC-conjugated goat anti-rabbit IgG (1:100) for 30 min at 37 degrees C. (A) Phase-contrast image of Day 10 stimulated human adipocyte at 20X. (B) Punctate APOC-I pattern on Day 10 stimulated human adipocytes. Imaged using fluorescein filter at 20X. (C) Day 10 human adipocyte control. Cells were incubated with only FITC-conjugated goat anti-rabbit IgG (1:100). All images taken with Zeiss Axioskop and Kodak MDS 290 imaging system at 20X objectives. All bars equal 50 μm.

3.6 Changes in Apolipoprotein C-I Detection in Treated Human Adipocytes

3.6.1 Effects of Heparinase Treatments

Differentiated human adipocytes were treated with heparinase (3 units/mL) and further imaged using immunofluorscence to determine potential APOC-I and heparan sulfate proteoglycan binding. First using phase-contrast microscopy at the 20X objective, Day 10 differentiated human adipocytes treated with heparinase exhibited the customary rounded cell-shape with plentiful lipid droplet formation (Figure 3.14a, b).

Fluorescent imaging of Day 10 heparinase-treated human adipocytes revealed a mixed effect: half of the cells exhibited a diffuse staining pattern while the remaining cells exhibited protein expression primarily on the periphery, or edge, of the cell, sometimes at focal-contact adhesion points on the plate (Figure 3.14c, d, e). Though APOC-I clusters occurred at the cell border, the pattern was not as distinct as the punctate pattern seen in the stimulated Day 10 fluorescent images. The control was a Day 10 heparinase and 0.5 % Triton-X 100 treated adipocyte cell incubated under the aforementioned conditions and exhibited the consistent diffuse pattern from Days 3 and 6 controls, though at a lesser fluorescent intensity (Figure 3.15).

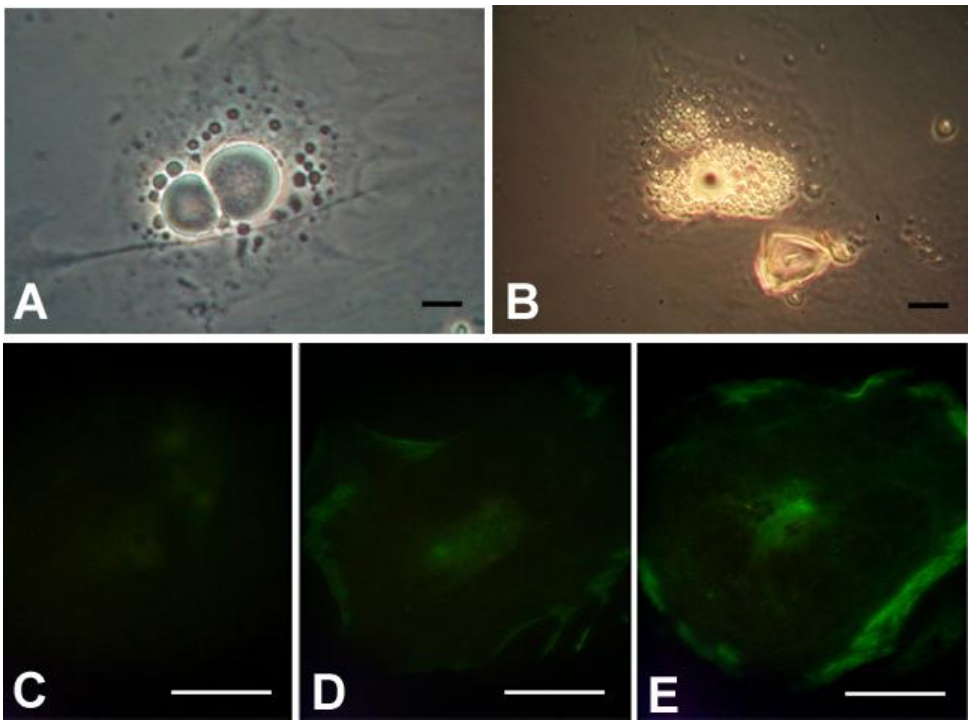

Figure 3.14. Heparinase-Treated Stimulated Day 10 Human Adipocytes.
Cells treated with 1mL of heparinase (3 units/mL) for 2 hours at 37C. After fixation, blocking, and washing, cells were incubated with rabbit anti-human APOC-I IgG (1:100) for 45 min at 37 degrees C, washed, and then incubated with fluorecein isothiocyanate conjugated goat anti-rabbit IgG (1:100) for 30 min at 37 degrees C. (A) Day 10 heparinase-treated adipocytes with lipid droplet accumulation. Phase-contrast image taken for 1/30 second. (C) Day 10 heparinase-treated adipocytes imaged using fluorescein filter for 2.0 s. Note absent APOC-I visualization. (D) and (E) Day 10 heparinase-treated adipocytes imaged using fluorescein filter for 2.0 s. Note varying degree of peripheral APOC-I accumulation. All bars equal 50 μm.

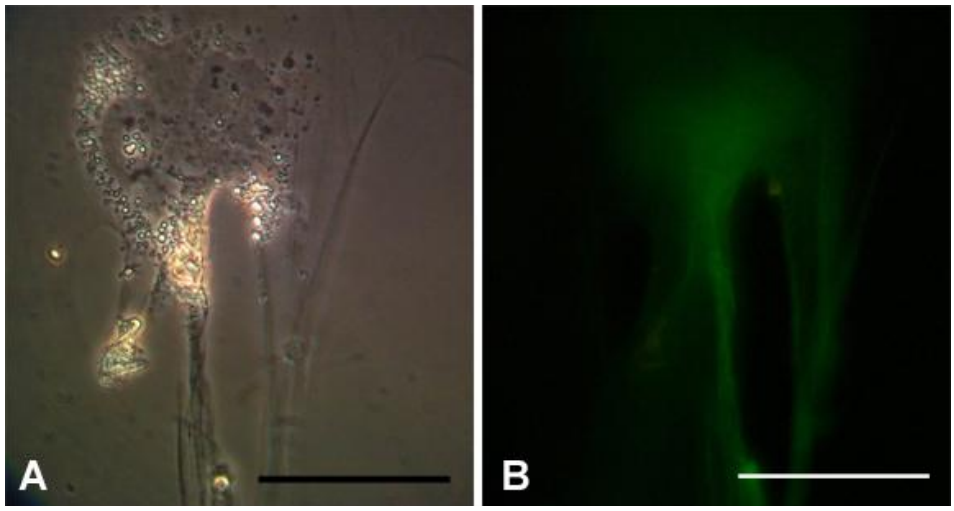

Figure 3.15. Heparinase and Triton-X 100 Treated Stimulated Day 10 Human Adipocytes Control. Cells were treated with heparinase (3 units/mL) for 2 hours at 37 degrees C. After fixing, cells were permeabilized with 0.5% Triton-X 100 for 5 mins at room temperature. Afterwards, cells were incubated with PBS-BSA (2%) for 45 mins at 37 degrees C and goat anti-rabbit-FITC conjugated antibody for 30 mins at 37 degrees C. (A) Phase-contrast image of Day 10 stimulated adipocyte with dual treatment. Note lipid droplet formation. (B) Immunofluorescent image of Day 10 stimulated adipocyte with dual treatment. Note diffuse background in cytoplasmic regions. All bars equal 50 μm.

3.6.2 Effects of Heparinase and Triton-X 100 Treatments

An additional treatment of 0.5% Triton-X 100 with heparinase was utilized to detect potential intracellular APOC-I. The combined treatment was conducted on Day 10 differentiated human adipocytes in addition to a control incubated in previously mentioned conditions. Phase contrast microscopy at 20X and 40X objectives of both treated and control cells revealed the indicated lipid droplet formation and canonical differentiated adipocyte cell morphology (Figure 3.15a, Figure 3.16a). Moreover, after treatment, immunofluorescent images revealed that APOC-I was not present in the

variegated manner reminiscent of Day 10 stimulated, untreated human adipocytes.

Instead, images showed diffuse, faint staining.

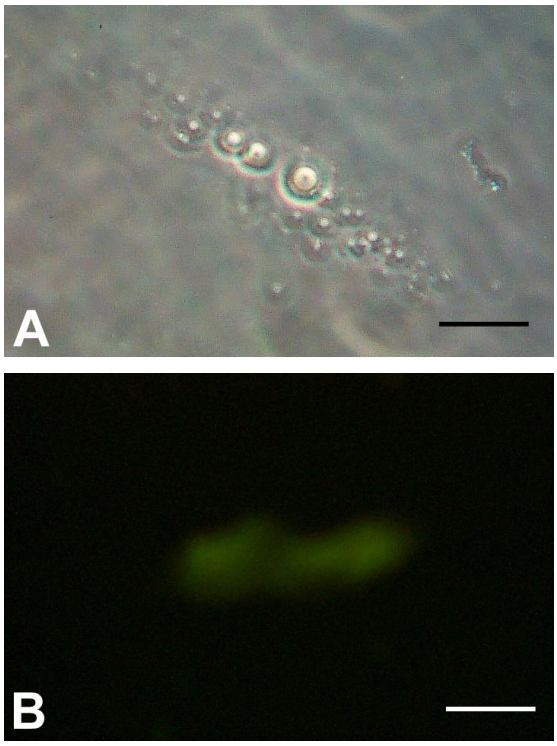

Figure 3.16. Heparinase and Triton-X 100 Treated Stimulated Day 10 Human Adipocytes Control. Cells were treated with heparinase (3 units/mL) for 2 hours at 37C. After fixing, cells were permeabilized with 0.5% Triton-X 100 for 5 mins at room temperature. Afterwards, cells were incubated with rabbit anti-human APOC-I antibody for 45 mins at 37C and goat anti-rabbit-FITC conjugated antibody for 30 mins at 37C. (A) Dual treated stimulated Day 10 human adipocyte. Note lipid droplet formation. Phase-contrast image taken at 40X objective for 1/30 second. (B) Same cell in *(a)*. Immunofluorescent image with fluorescein filter at 40X objective. All bars equal 50 μm.

Chapter 4

DISCUSSION

Cholesterol efflux, the process in which extrahepatic cells export intracellular unesterified cholesterol to the cell surface, involves a myriad of proteins and lipoprotein particles, though the exact mechanism is not well understood. Current research has demonstrated, though, that cells produce and secrete specific aplipoproteins to aid in cholesterol efflux. For example, the well-studied apolipoprotein E produced by macrophages, hepatocytes, glial cells, and adipocytes interacts with the transmembrane ABCA1 to shuttle cholesterol from the peripheral cell to the extracellular lipoprotein cholesterol acceptor (Mahley, Huang, & Weisgraber, Putting cholesterol in its place: apoE and reverse cholesterol transport, 2006). Another less-studied apolipoprotein, apoC-I, has also been shown to play a role in cholesterol efflux, specifically in mice macrophages *in vitro* (Westerterp et al., 2007). The Usher Lab had previously determined that *Apoe* and *Apoc1* mRNA levels are highly upregulated during mouse adipocyte differentiation, and are, moreover, sensitive to intracellular cholesterol levels. Thus, the aim of this study was to verify prior *Apoc1* and *Apoe* mRNA results in mouse 3T3-L1 cells and also to determine APOC-I production and secretion in human adipocytes.

QPCR used to detect mouse *Apoe* and *Apoc1* mRNA levels confirmed findings from previous studies conducted in the Usher Lab, although data included much lower mRNA levels than prior studies. *Apoe* and *Apoc1* mRNA levels were upregulated during mouse 3T3-L1 adipocyte differentiation, with *Apoc1* being activated as a late-phase gene on Day 6 of differentiation. The results found in previous studies as well as this one demonstrated that *Apoe* mRNA expression is highest on Day 3, or intermediate-phase differentiation, rather than late-phase differentiation.

Regarding *Apoe* and *Apoc1* mRNA expression in response to intracellular cholesterol levels, similar results were obtained as prior studies conducted in the Usher Lab, thereby verifying previous data. The first treatment was the LXR agonist T0901317, an oxysterol derivative shown to induce LXR production and thus mimic intracellular cholesterol abundance. QPCR results showed upregulated *Apoe* and *Apoc1* mRNA expression, demonstrating that *Apoc1 and Apoe* are sensitive to LXR control. Moreover, *Apoc1* was more affected by the LXR agonist than *Apoe,* suggesting that *Apoc1* may be more responsive to cholesterol abundance. The second treatment of β-cylcodextrin and HDL, used to cholesterol-depleted mouse adipocytes, was not as effective as in prior studies. For instance, *Apoe* mRNA levels did not exhibit a significant drop, although *Apoc1* mRNA levels decreased more drastically.Thus, *Apoc1* mRNA levels were most affected by the cholesterol depletion treatments, similar to previous findings in the Usher Lab, though at much lower mRNA levels (unpublished, David, 2006). Lastly, because the combined treatment of LXR stimulation and cholesterol depletion induced even greater *Apoe* and *Apoc1*

mRNA expression than LXR agonist alone, results were not similar to previously found data and may be due to aberrant cholesterol depletion treatments.

Regardless, since LXR stimulation and cholesterol depletion affected *Apoe* and *Apoc1* mRNA expression compared to stimulated controls, results suggest that both genes, then, play a role in dictating adipocyte size. Cholesterol comprises the lipid bilayer membrane and forms the lipid droplet boundary in adipocytes; thus, expression of potential cholesterol efflux apolipoproteins like apoC-I would potentially affect cholesterol balance and thus dictate adipocyte size. Additionally, if apoC-I is involved in cholesterol efflux, then it should also be expressed on the cell surface, like apoE, to associate with various extracellular lipoprotein acceptors. Since apoE has been shown to be produced by mouse and human adipocytes, the remainder of the study was focused on elucidating human APOC-I production in differentiated human subcutaneous adipocytes. Viable mouse anti-apoC-I antibodies were tested for specificity but not used (data not shown).

Since APOE production has been well-documented in hepatocytes, macrophages, glial cells (Koistinaho, et al., 2004), and adipocytes, attempts to detect APOC-I production in adipocytes mirrored current APOE methodologies (Carmel, Tarnus, Cohn, Bourdon, Davignon, & Bernier, 2009). In adipocytes, specifically, APOE is secreted as a water-soluble protein prior to re-entry into the cell and glycosylation in the Gogli apparatus. Moreover, ELISA assays conducted by the Usher Lab revealed that APOC-I concentration in the supernatant of a T-75 flask containing human adipocytes was about 4.5 ng/mL (unpublished, David, 2006), which is significant

considering the normal circulating levels of APOC-I is 6 mg/dL (Cohn, et al., 2003). The subsequent slot-blot assay of various fractions from mature human subcutaneous adipocyte supernatant showed that APOC-I associated with the top fraction, or the lipoprotein fraction, and with the bottom fraction. The results of the slot-blot suggested that, as hypothesized, APOC-I was associating with lipoproteins; however, since it also was found in the bottom fraction, it may be that APOC-I is being secreted and not binding to extracellular lipoprotein particles. Western blot analysis of top fractions collected during the entire adipocyte differentiation time-course revealed no APOC-I production, however. Although supernatant samples were loaded as 1 ug of protein per mL, low detection could be due to low APOC-I concentrations. Western blot results suggest that APOC-I is either not being produced during late-phase adipocyte differentiation—which would disagree with the high mRNA levels, or is secreted in undetectable amounts, or like APOE, it is being secreted and mostly attaching to the adipocyte cell surface.

Literature has revealed that APOE, in addition to being secreted as a water-soluble protein in the extracellular environment, binds to heparan sulfate proteoglycans (Burgess, Gould, & Marcel, The HepG2 Extracellular Matrix Contains Separate Heparinase- and Lipid-releasable Pools of ApoE, 1998). Since western blot analyses revealed no APOC-I secretion in human adipocyte supernatants and the protein structure revealed plentiful potential binding sites for heparan sulfate proteoglycans, it was hypothesized that APOC-I may bind in a similar manner. Specifically, lysine and arginine spanning the 136-150 residues in APOE were identified as the major amino

acids interacting with N-, 2-O, and 6-O-sulfo groups in glucosamine residues on heparan sulfate chains; similar residues were found in APOC-I, and interestingly, at a higher percentage than in APOE. Immunoflourescence of stimulated human adipocytes demonstrated that no APOC-I was detectable on the cell surface during early- and intermediate-phase differentiation. But at Day 6, or late-phase differentiation, APOC-I was visualized on the cellular surface in a distinct punctuate pattern. The punctuate APOC-I characterization fits accordingly to current postulations regarding HSPG cell membrane dispersion. Heparan sulfate chains attaches primarily to the transmembrane protein syndecan, which clusters in cell-surface microdomains or associates with possible lipid rafts. Both types of associations could explain the punctuate pattern found with APOC-I. Moreover, the most convincing conclusions came from the post-heparinase treatment immunofluorescent images (Figure 3.14, Figure 3.16).

Upon heparinase treatment and a combination of heparinase and cell permeabilization treatments, APOC-I was no longer seen in the same speckled distribution on the adipocyte surface. Rather, following heparinase treatments, APOC-I was gathered at the periphery of the cell, specifically at the cell-cover slip interface. The resulting staining pattern may be because the dissociated APOC-I was incompletely washed from the glass cover slip and was therefore visualized solely at the cell periphery, suggesting the detected APOC-I in post-heparinase treatments was artifactual. However, the possibility that APOC-I interacts with other non-HSPG molecules on the cell surface, specifically at the cell-cover slip border, was

entertained. Current research has shown that macrophage-secreted APOE can associate with chondroitin sulfate chains along with HSPG-interactions, which may explain additional APOC-I staining (Burgess, Liang, Vaidyanath, & Marcel, 1999). However, that postulation was tentatively ruled out since stimulated Day 10 immunoflourescence images did not contain the same marked APOC-I gathering at the cellular edges. Ultimately, after heparinase treatments a clear difference was seen between stimulated and heparinase-treated cells. Moreover, heparinase combined with Triton-X 100 yielded expected results and showed a lack of punctate APOC-I distribution with, instead, a diffuse immunofluorescent background.

APOC-I-HSPG associations on the human adipocyte surface suggest that APOC-I may associate with said hypothetical lipid rafts and, moreover, (1) act as a cholesterol acceptor in cholesterol efflux if endogenously produced or (2) act as a lipoprotein acceptor, thereby mediating cellular lipoprotein uptake, if associated with exogenous HDL. Although the existence of lipid rafts has come into question recently, other studies have confirmed their presence by confocal laser scanning microscopy, fluorescence resonance energy transfer microscopy, atomic force microscopy, transmission electron microscopy coupled with immunogold labeling, or membrane patch-clamping techniques (Matko & Szollosi, 2005). Regardless, assuming that lipid rafts exist, as aforementioned APOC-I binding to heparan sulfate—associated with primarily syndecan located in lipid rafts—suggests APOC-I's role in cholesterol efflux if it is endogenously produced. For instance, it is hypothesized that transmembrane proteins ABCA1 and ABCG1 associate with lipid rafts (Koseki, et al., 2007). Since

ABCA1 and ABCG1 have been shown to facilitate cholesterol efflux to extracellular lipoprotein acceptors like HDL (Gaus, Gooding, Dean, Kritharides, & Jessup, 2001) it is possible, since APOC-I is localized with rafts, that APOC-I associates with the ABC transporters in microdomains to facilitate cholesterol efflux as well.

Moreover, APOC-I-HSPG associations on the human adipocyte surface suggest that APOC-I not only facilitates cellular cholesterol efflux but, if exogenously expressed on lipoprotein particles, it may also aid in lipoprotein uptake through associated lipid rafts, similar to APOE. Mouse apoE is known to associate with LRPs and LDLRs expressed on the liver through HSPG binding (Attie & Seidah, 2005); specifically, apoE-bound HSPG assists hepatic uptake of remnant particles by either independently binding lipoprotein remnants or by facilitating remnant particle-LRP binding (Mahley & Huang, Atherogenic remnant lipoproteins: role for proteoglycans in trapping, transferring, and internalizing, 2007). This was also suggested in one study conducted by MacArthur et al. (2007); sulfation of hepatic heparan sulfate was reduced by inactiving the biosynthestic gene *GlcNAcN-deacteylase/N-sulfotransferase 1 (Ndst1)* and the subsequent knock-down of heparan sulfate proteoglycans resulted in mice with severe lipoproteinemia, or increased accumulation of triglyceride- and cholesterol-rich lipoprotein particles expressing apoB-100, apoB-48, apoE, and apoC-I to apoC-IV. Additionally, when the mutation was compounded with the knock-out LDLR $^{-/-}$ phenotype, mice exhibited significantly enhanced circulatory lipoprotein accumulation (MacArthur, et al., 2007). Another study used mice homozygous for an apoE variant [apoE(R142C)] which exhibits impaired HSPG binding (<5% of apoE3

activity) (Horie, 1992). Transgenic mice were unable to clear lipoprotein remnants in the sinusoidal spaces of Disse because of impaired LDLR and LRP binding, suggesting that HSPG-apoE interactions are necessary in hepatic clearance of lipoprotein remnants. Ultimately, since apoE-HSPG binding on the cell-surface proves important in lipoprotein clearance and cellular cholesterol uptake, apoC-I expression on the adipocyte surface may function to enhance cellular uptake of extracellular lipoprotein particles. Additionally, APOC-I has also been shown to bind with higher affinity to APOE-associated receptors; it may, therefore, bind to lipoprotein acceptors with a higher affinity than APOE.

Since APOC-I associates with HSPG like APOE, and perhaps with a higher binding affinity, APOC-I may disrupt APOE-HSPG interactions, ultimately modulating cellular lipoprotein uptake. In vitro assays have shown that APOC-I interferes with APOE-mediated binding to LDLR (Sehayek, 1991) as well as APOE-mediated LRP binding (Weisgraber K. , Mahley, Kowal, Herz, Goldstein, & Brown, 1990). Some research suggests that APOC-I conformationally changes APOE or that it competitively binds to said receptors which is not surprising since APOC-I contains a much higher percentage of lysine residues than APOE. Polylysine proteins are capable of ubiquitous hydrogen bonding to negatively charged surfaces, like hyper-sulfated HSPGs; this suggests that APOC-I could bind with higher affinity to HSPGs than APOE. If that is the case then because of its antagonistic character, it may competitively bind to various cholesterol acceptors. A speculation then is that lipoprotein-associated APOC-I interacts with HSPGs in lipid rafts with a higher

affinity than APOE and modulates cellular lipoproprotein uptake. Ultimately, then, in adipocytes this would affect adipocyte intracellular cholesterol content, thereby dictating adipocyte size.

In adipocytes, specifically, this competitive binding would be important in adipose tissue re-modeling. Studies with obese mice (*obob* mice) overexpressing human APOC-I (either APOC-I $^{+/+}$ or APOC-I $^{+/-}$) resulted in severely reduced subcutaneous adipose tissue because of diminished net uptake of free fatty acids (Muurling, et al., 2004).Moreover, *obob*/APOC-I $^{+/+}$ mice showed less adipose tissue than heterozygous APOC-I mice, which demonstrates that varying degrees of APOC-I overexpression dictates adipose tissue mass (Jong, et al., 2001). Therefore, if APOC-I is produced by adipocytes and binds competitively with various cholesterol acceptors, it may serve to regulate cholesterol levels within adipocytes, thereby dictating adipocyte size and remodeling adipose tissue.

In conclusion, this study first verified previous work conducted on *Apoe* and *Apoc1* mRNA expression in mouse 3T3-L1 cells; specifically, *Apoe* mRNA was shown to peak on Day 3 of differentiation while *Apoc1* mRNA was most expressed on Day 6 of differentiation, or late-phase adipocyte differentiation. Moreover, *Apoe* and *Apoc1* mRNA expression was shown to be sensitive to intracellular cholesterol levels in mice. The second aim of the study was to detect APOC-I production in human adipocytes. It was determined that APOC-I is produced during late-phase adipocyte differentiation and associates with cell surface HSPGs. The verification and possible

role of adipocyte-secreted APOC-I and its attachment to hypothesized lipid rafts through HSPGs interactions remains to be determined.

REFERENCES

Abildayeva, K., Berbee, J. F., Blokland, A., Jansen, P. J., Hoek, F. J., Meijer, O., et al. (2008). Human apolipoprotein C-I expression in mice impairs learning and memory functions. *Journal of Lipid Research* , 856-869.

Adorni, M. P., Zimetti, F., Billheimer, J., Wang, N., Rader, D. J., Phillips, M. C., et al. (2007). The roles of different pathways in the release of cholesterol from macrophages. *Journal of Lipid Research* , 2453-2463.

Attie, A. D., & Seidah, N. G. (2005). Dual regulation of the LDL receptor—Some clarity and new questions. *Cell Metabolism, 1* (5), 290-292.

Bays, H. E. (2009). "Sick Fat," Metabolic Disease, and Atherosclerosis. *The American Journal of Medicine , 122* (1), S26-S37.

Brasaemle, D. L. (2007). Thematic review series: Adipocyte Biology. The perilipin family of structural lipid droplet proteins: stabilization of lipid droplets and control of lipolysis. *Journal of Lipid Research, 48,* 2547-2559.

Burgess, J. W., Gould, D. R., & Marcel, Y. (1998). The HepG2 Extracellular Matrix Contains Separate Heparinase- and Lipid-releasable Pools of ApoE. *Journal of Biological Chemistry* , 5645-5654.

Burgess, J. W., Liang, P., Vaidyanath, C., & Marcel, Y. L. (1999). ApoE of the HepG2 Cell Surface Includes a Major Pool Associated with Chondroitin Sulfate Proteoglycans. *Biochemistry* , 524-531.

Carmel, J., Tarnus, E., Cohn, J., Bourdon, E., Davignon, J., & Bernier, L. (2009). High expression of apolipoprotein E impairs lipid storage and promotes cell proliferation in human adipocytes. *Journal of Cell Biochemistry , 106* (4), 608-617.

Cohn, J., Batal, R., Tremblay, M., Jacques, H., Veilleux, L., Rodriguez, C., et al. (2003). Plasma Turnover of HDL ApoC-I, ApoC-III and ApoE in Humans: in vivo evidence for a link between HDL apoC-III and apoA-I metabolism. *Journal of Lipid Research* , 1976-1983.

David, J. (2006). The Control of Apolipoprotein C-I Gene Expression During Adipocyte Differentiation. *Master's Thesis* . Newark, Delaware: University of Delaware.

de la Llera-Moya, M., Connelly, M. A., Drazul, D., Klein, S. M., Favari, E., Yancey, P. G., et al. (2001). Scavenger receptor class B type I affects cholesterol homeostasis by magnifying cholesterol flux between cells and HDL. *Journal of Lipid Research* , 1969-1978.

Dove, D. E., Linton, M., & Fazio, S. (2004). ApoE-mediated cholesterol efflux from macrophages: separation of autocrine and paracrine effects. *American Journal of Cell Physiology* , C586-C592.

Ducharme, N. A., & Bickel, P. E. (2008). Minireview: Lipid Droplets in Lipogenesis and Lipolysis. *Endocrinology , 149* (3), 942-949.

Gaus, K., Gooding, J. J., Dean, R. T., Kritharides, L., & Jessup, W. (2001). A Kinetic Model to Evaluate Cholesterol Efflux from THP-1 Macrophages to Apolipoprotein A-1. *Biochemistry* , 9363-9373.

Gautier, T., Masson, D., Jong, M. C., Duverneuil, L., Guern, N. L., Deckert, V., et al. (2002). Apolipoprotein CI Deficiency Markedly Augments Plasma Lipoprotein Changes Mediated by Human Cholesteryl Ester Transfer Protein (CETP) in CETP Transgenic/ApoCI-knocked Out Mice. *Journal of Biological Chemistry* , 31354-31363.

Gautier, T., Masson, D., Pais de Barros, J.-P., Athias, A., Gamber, P., Aunis, D., et al. (2000). Human apolipoprotein C-I accounts for the ability of plasma high density lipoproteins to inhibit the cholesteryl ester transfer protein activity. *Journal of Biological Chemistry* , 37504-37509.

Gelissen, I. C., Harris, M., Rye, K.-A., Quinn, C., Brown, A. J., Kockx, M., et al. (2006). ABCA1 and ABCG1 Synergize to Mediate Cholesterol Export to ApoA-I. *Arteriosclerosis, Thrombosis, and Vascular Biology* , 534-540.

Ha, Y. C., & Barter, P. J. (1985). Differences in plasma cholesteryl ester transfer protein in sixteen vertebrate species. *Comp. Biochem. Physiol.* , 265-269.

Hadri, K., Glorian, M., Monsempes, C., Dieudonne, M.-N., Pecquery, R., Giudicelli, Y., et al. (2004). In Vitro Suppression of the Lipogenic Pathway by the

Nonnucleoside Reverse Transcriptase Inhibitor Efavirenz in 3T3 and Human Preadipocytes or Adipocytes. *Journal of Biological Chemistry* , 15130-15141.

Haslam, D. W., & James, P. W. (2005). Obesity. *The Lancet , 366* (9492), 1197-1209.

Hoeg, J. M., Vaisman, B. L., Demosky Jr., S. J., Meyn, S. M., Talley, G. D., Hoyt Jr., R. F., et al. (1996). Lecithin:Cholesterol Acyltransferase Overexpression Generates Hyperalpha-lipoproteinemia and a Nonatherogenic Lipoprotein Pattern in Transgenic Rabbits. *American Society for Biochemistry and Molecular Biology* , 4396-4402.

Horie, Y. F. (1992). The functional characteristics of a human apolipoprotein E variant (cysteine at residue 142) may explain its association with dominant expression of type III hyperlipoproteinemia. *Journal of Biological Chemistry* , 1962-1968.

Huang, Z. H., Lin, C.-Y., Oram, J. F., & Mazzone, T. (2001). Sterol Efflux Mediated by Endogenous Macrophage ApoE Expression Is Independent of ABCA1. *Arteriosclerosis, Thrombology, and Vascular Biology* , 2019-2025.

Imamura, M., Inoguchi, T., Ikuy, S., Taniguchi, S., Kobayashi, K., Nakashima, N., et al. (2002). ADRP stimulates lipid accumulation and lipid droplet formation in murine fibroblasts. *Am J Physiology: Endocrinology and Metabolism* , E775-E783.

Inoue, J., Kumagai, H., Terada, T., Maeda, M., Shimizu, M., & Sato, R. (2001). Proteolytic activation of SREBPs during adipocyte differentiation. *Biochem Biophys Res Commun.* , 1157-1161.

Ji, Z.-S., Brecht, W. J., Miranda, D., Hussain, M. M., Innerarity, T. L., & Mahley, R. W. (1993). Role of Heparan Sulfate Proteoglycans in the Binding and Uptake of Apolipoprotein E-enriched Remnant Lipoproteins by Cultured Cells. *Journal of Biological Chemistry* , 10160-10167.

Jong, M. C., Hofker, M. H., & Havekes, L. M. (1999). Role of ApoCs in Lipoprotein Metabolism. *Arteriosclerosis, Thrombosis, and Vascular Biology* , 472-484.

Jong, M., Voshol, P., Muurling, M., Dahlmans, V., Romijn, J., Pijl, H., et al. (2001). Protection from obesity and insulin resistance in mice overexpressing human apolipoprotein C-I. *Diabetes* , 2779-2785.

Koistinaho, M., Lin, S., Wu, X., Esterman, M., Koger, D., Hanson, J., et al. (2004). Apolipoprotein E promotes astrocyte colocalization and degradation of deposited amyloid-beta peptides. *Nature Medicine* , 719-726.

Koseki, M., Hirano, K., Masuda, D., Ikegami, C., Tanaka, M., Ota, A., et al. (2007). Increased lipid rafts and accelerated lipopolysaccharide-induced tumor necrosis factor-alpha secretion in Abca1-deficient macrophages. *Journal of Lipid Research* , 299-306.

Kowal, R., Herz, J., Weisgraber, K., Mahley, R., Brown, M., & Goldstein, J. (1990). Opposing effects of apolipoproteins E and C on lipoprotein binding to low density lipoprotein receptor-related protein. *Journal of Biological Chemistry* , 10771-10779.

Laffitte, B. A., Repa, J. J., Joseph, S. B., Wilpitz, D. C., Kast, H. R., Mangelsdorf, D. J., et al. (2001). LXRs control lipid-inducible expression of the apolipoprotein

E gene in macrophages and adipocytes. *Proceedings of the National Academy of Science of the United States of America* , 507-512.

Le Lay, S., Ferre', P., & Dugail, I. (2004). Adipocyte cholesterol balance in obesity. *Biochemical Society Transactions , 32* (1), 103-106.

Libeu, C. P., Lund-Katz, S., Phillips, M. C., Wehrli, S., Hernaiz, M. J., Capila, I., et al. (2001). New Insights into the Heparan Sulfate Proteoglycan-binding Activity of Apolipoprotein E. *Journal of Biological Chemistry* , 39138-39144.

Lilly-Stauderman, M., Brown, T. L., Balasubramaniam, A., & Harmony, J. A. (1993). Heparin releases newly synthesized cell surface-associated apolipoprotein E from HepG2 cells. *Journal of Lipid Research* , 190-200.

Listenberger, L. L., Ostermeyer-Fay, A. G., Goldberg, E. B., Brown, W. J., & Brown, D. A. (2007). Adipocyte differentiation-related protein reduces the lipid droplet association of adipose triglyceride lipase and slows triacylglycerol turnover. *Journal of Lipid Research , 48,* 2751-2761.

Lucas, M., & Mazzone, T. (1996). Cell Surface Proteoglycans Modulate Net Synthesis and Secretion of Macrophage Apolipoprotein E. *American Society for Biochemsitry and Molecular Biology , 271* (23), 13454-13460.

MacArthur, J. M., Bishop, J. R., Stanford, K. I., Wang, L., Bensadoun, A., Witztum, J. L., et al. (2007). Liver heparan sulfate proteoglycans mediate clearance of triglyceride-rich lipoproteins independently of LDL receptor family members. *Journal of Clinical Investigation* , 153-164.

Mahley, R. W., & Huang, Y. (2007). Atherogenic remnant lipoproteins: role for proteoglycans in trapping, transferring, and internalizing. *Journal of Clinical Investigation* , 94-98.

Mahley, R. W., Huang, Y., & Weisgraber, K. H. (2006). Putting cholesterol in its place: apoE and reverse cholesterol transport. *Journal of Clinical Investigation* , 1226-1229.

Matko, J., & Szollosi, J. (2005). Regulatory Aspects of Membrane Microdomain (Raft) Dynamics in Live Cells: A Biophysical Approach. In M. P. Mattson, *Membrane Microdomain Signaling: Lipid Rafts in Biology and Medicine* (pp. 15-46). Totowa: Humana Press.

Muurling, M., van den Hoek, A. M., Mensink, R. P., Pijl, H., Romijn, J. A., Havekes, L. M., et al. (2004). Overexpression of APOC1 in obob mice leads to hepatic steatosis and severe hepatic insulin resistance. *Journal of Lipid Research* , 9-16.

Nguyen, D., Dhanasekaran, P., Phillips, M. C., & Lund-Katz, S. (2009). Molecular Mechanism of Apolipoprotein E Binding to Lipoprotein Particles. *Biochemistry* , 3024-3032.

Petit-Turcotte, C., Stohl, S. M., Beffert, U., Cohn, J. S., Aumont, N., Tremblay, M., et al. (2001). Apolipoprotein C-I Expression in the Brain in Alzheimer's Disease. *Neurobiology of Disease* , 953-963.

Radhakrishnan, A., Goldstein, J. L., McDonald, J. G., & Brown, M. S. (2008). Switch-like Control of SREBP-2 Transport Triggered by Small Changes in ER Cholesterol: A Delicate Balance. *Cell Metabolism* , 512-521.

Sehayek, E. a. (1991). Mechanisms of inhibition by apolipoprotein C of apolipoprotein E-dependent cellular metabolism of human triglyceride-rich lipoproteins through the low density lipoprotein receptor. *Jounral of Biological Chemistry* , 18259-18267.

Sterling, S. E. (2007). Cholesterol Homeostasis in Adipocytes. *Senior Thesis* . Newark, Delaware: University of Delaware.

Weisgraber, K. H., & Mahley, R. W. (1996). Human apolipoprotein E: the Alzheimer's disease connection. *FASEB Journal* , 1485-1494.

Weisgraber, K., Mahley, R., Kowal, R., Herz, J., Goldstein, J., & Brown, a. M. (1990). Apolipoprotein C-I modulates the interaction of apolipoprotein E with B-migrating very low density lipoproteins (B-VLDL) and inhibits binding of B-VLDL to low density lipoprotein receptor-related protein. *Journal of Biological Chemistry* , 22453-22459.

Westerterp, M., Van Eck, M., de Haan, W., Offerman, E. H., Van Berkel, T. J., Havekes, L. M., et al. (2007). Apolipoprotein CI aggravates atherosclerosis development in ApoE-knockout mice despite mediating cholesterol efflux from macrophages. *Atherosclerosis* , e9-e16.

Yancey, P. G., Bortnick, A., Kellner-Weibel, G., de la Llera-Moya, M., Phillips, M. C., & Rothblat, G. H. (2003). Importance of Different Pathways of Cellular

Cholesterol Efflux. *Ateriosclerosis, Thrombosis, and Vascular Biology* , 712-719.

Yang, T., Espenshade, P., Wright, M., Yabe, D., Gong, Y., Aebersold, R., et al. (2002). Crucial step in cholesterol homeostasis: sterols promote binding of SCAP to INSIG-1, a membrane protein that facilitates retention of SREBPs in ER. *Cell* , 489-500.

Yue, Y., & Ginsberg, H. N. (2005). Adipcoyte signaling and lipid homeostasis: sequelae of insulin-resistant adipose tissue. *Circulation Research* , 1042-1052.

Zechner, R., Moser, R., Newman, T. C., Fried, S. K., & Breslow, J. L. (1990). Apolipoprotein E Gene Expression in Mouse 3T3-Ll Adipocytes. *Journal of Biological Chemistry* , 10683-10688.

Zeng, L., Liao, H., Liu, Y., Lee, T.-S., Zhu, M., Wang, X., et al. (2001). Sterol-responsive Element-binding Protein (SREBP) 2 down-regulates ATP-binding Cassette Transporter A1 in vascular endothelial cells. *Journal of Biological Chemistry* , 48801-48807.